

THE ROLE OF ALTERED MICRORNA EXPRESSION IN AN EXPERIMENTAL MODEL
OF ESTROGEN-DEPENDENT UTERINE CANCER

A Thesis by

Ramesh Padmanabhan

Master of Science, Bharathiar University, Coimbatore, India, 2004

Submitted to the Department of Biological Sciences
and the faculty of the Graduate School of
Wichita State University
in partial fulfillment of
the requirements for the degree of
Master of Science

July 2009

© Copyright 2009 by Ramesh Padmanabhan

All Rights Reserved

THE ROLE OF ALTERED MICRORNA EXPRESSION IN AN EXPERIMENTAL MODEL
OF ESTROGEN-DEPENDENT UTERINE CANCER

The following faculty members have examined the final copy of the thesis for form and content and recommend that it be accepted in partial fulfillment of the requirements for the degree of Master of Science with a major in Biological Sciences.

William J Hendry, Committee Chair

Bin Shuai, Committee member

Kandatege Wimalasena, Committee member

DEDICATION

To my parents, my grand parents, and my sister

ACKNOWLEDGEMENTS

I feel highly privileged to express my deep sense of gratitude and profound thanks to my graduate advisor, Dr. William J Hendry, Ph.D. for his able guidance, timely motivation, and advice and for mentoring me toward my future career. Without his constant advice, it would have been arduous for me to complete this research.

I offer my profound thanks to my committee members: Drs Bin Shuai and Kandatege Wimalasena for their continuous support and insightful comments. Special thanks to Dr. Bin Shuai for letting me use her lab for real-time PCR and helping me at various stages of the procedure.

I owe my sincere thanks to Isabel Hendry for all her valuable advice as well as offering her seasoned suggestions on different techniques I used for my research. I extend my appreciation to Maria for all her help with administrative matters pertaining to the Master's program at Wichita State University and for her valuable and timely advice. My word of thanks to all the fellow graduate students in the Department of Biological sciences, especially Mr. Shane McIntyre and Ms. Megan Simpson, for all the help they rendered me in completing this project successfully.

On a personal note, I ardently express my indebtedness and gratitude to my parents, sister, and Brother-in-law without whose generous sacrifice, magnanimity, and unstinted encouragement and inspiration, this project work could not have seen the light of day. Last but not least, my prayers to the Almighty who gave me the strength and blessings to successfully complete my research.

ABSTRACT

This project screened for altered expression of small RNA species, microRNAs (miRNA), in the hamster uterus following neonatal exposure to the potent synthetic estrogen and established endocrine disruptor diethylstilbestrol (DES). Neonatal DES exposure results in a dysplastic/neoplastic response of the adult hamster uterus to the natural ovarian estrogen, estradiol (E2). In the present study, miRNA profiling was performed with total RNA extracted from the uteri of control and neonatally DES-treated female hamsters. We exploited a highly sensitive, reliable, and accurate microarray profiling technology and used it to screen for the differential expression of miRNA genes during both the initiation and promotion stages of estrogen-dependent endometrial adenocarcinoma in the neonatally DES-treated hamster. MiRNAs that were two-fold or more differentially expressed in DES-treated animals compared with the control animals were validated using a sensitive and highly specific quantitative RT-PCR technique. In the initiation stage a total of eight miRNAs including the miR-200 family members miR-200a, miR-200b, miR-200c, miR-141 and miR-429; miR-29a/b and miR-21 that is found altered in many cancers were up-regulated more than 2-fold; and one miRNA, miR-181a, was down-regulated by more than 2-fold. However, there was only a single down-regulated miRNA, miR-133a, at the 2-month old promotion stage. These results were validated by the qRT-PCR assays. The change in miRNA expression was expressed as ΔC_T values \pm standard error of means (SEM) with statistical significance assessed by student's t-test ($p < 0.05$). The results suggest that the molecular mechanism of neonatal DES-induced uterine dysplasia/neoplasia in the hamster involves altered expression of specific miRNAs; perhaps more importantly during the initiation than the promotion stage of the phenomenon.

TABLE OF CONTENTS

Chapter		Page
1	INTRODUCTION AND BACKGROUND	1
1.1	Gene Expression and Regulation	1
1.2	A Brief History of miRNA Discovery	3
1.3	Biogenesis of miRNA	4
1.4	Relevance of miRNAs To Physiology and Disease	4
1.4.1	Age- Related Diseases	5
1.4.2	Cardiac Development and Cardiac Excitability.....	6
1.4.3	MiRNAs in Brain Development and Diseases.....	7
1.4.4	MiRNAs in Inflammation and Immune System	8
1.4.5	MiRNA Expression in Endometriosis	9
1.5	MiRNAs and Cancer	10
1.6	MiRNA Profiling Classifies Cancer Types	12
1.7	MiR-21: A miRNA Up- Regulated in Cancers	14
1.8	Inhibition of MiRNAs as New Therapeutic Strategy.....	15
1.9	Endocrine Disruption and DES Exposure	16
1.10	Specific Aims and Hypothesis of the Study.....	17
2	MATERIALS AND METHODS.....	19
2.1	Animals	19
2.2	Experimental Design	19
2.3	Total RNA Isolation	20
2.4	MiRNA Profiling.....	21
2.5	Validation of the Profiling Results by Quantitative Real-Time PCR	21
3	RESULTS	27
3.1	Total RNA Isolation	27
3.2	Total RNA Quality Control.....	30
4	CONCLUSION AND FUTURE DIRECTIONS.....	55
	LIST OF REFERENCES	60

LIST OF TABLES

Table	Page
1. Tissue weights and volume of lysis buffer added for initiation stage.....	20
2. Tissue weights and volume of lysis buffer added for promotion stage.....	20
3. Reverse transcription reaction components.....	24
4. Reverse transcription parameters.....	25
5. Real-time cocktail components.....	25
6. Real-time PCR parameters.....	26
7. Spectrophotometer reading for total RNA.....	27
8. RIN number and rRNA ratio for total RNA samples from initiation stage.....	33
9. RIN number and rRNA ratio for total RNA samples from promotion stage.....	34
10. Chip barcodes for NU and initiation stage.....	34
11. Chip barcodes for NU and promotion stage.....	35
12. Fold-change data for initiation stage.....	41
13. Fold-change data for promotion stage.....	46
14. ΔC_T values +/- SEM (>2-fold difference).....	51
15. ΔC_T values +/- SEM (>2-fold difference).....	53

LIST OF FIGURES

Figure	Page
1. Two-step RT-PCR assay.....	23
2. Total RNA extracted from normal hamster uterus analyzed in 1% agarose gel	28
3. Total RNA extracted from initiation stage samples analyzed in 1% agarose gel.....	29
4. Total RNA extracted from promotion stage samples analyzed in 1% agarose gel.....	30
5. Electropherogram for total RNA samples.....	31
6. Bioanalyzer 2100 data for NU and initiation stage samples.....	32
7. Bioanalyzer 2100 data for NU and promotion stage samples.....	33
8. Scatter plots for pair-wise comparison of miRNA hits for set “I”.....	37
9. Scatter plots for pair-wise comparison of miRNA hits for set “P”.....	38
10. Hierarchical clustering with Z-transformed signals for set “I”.....	39
11. Hierarchical clustering with Z-transformed signals for set “P”.....	39
12. miRNA expression in total RNA samples from control and DES- exposed uteri shown as Δ CT values.....	52
13. MiR-10b and miR-130b expression in total RNA samples from control and DES-exposed uteri shown as Δ CT Values.....	53
14. Comparison of fold-change differences between miRNA microarray and TaqMan miRNA RT-PCR assay.....	54

LIST OF ABBREVIATIONS

µg	Micrograms
3'-UTRs	3'-Untranslated Regions
AMO	Anti-miRNA oligonucleotide
Bp	Base pairs
cDNA	Complementary DNA
CNS	Central Nervous system
Ct	Threshold cycle
DES	Diethyl Stilbestrol
DGCR8	DiGeorge Syndrome Critical Region 8
DLBCL	Diffuse Large B-Cell Lymphoma
DNA	Deoxyribo Nucleic Acid
dsRNA	Double stranded RNA
GTP	Guanosine tri-phosphate
EMT	Epithelial-mesenchymal transition
hCLL	Human Chronic LymphocyticLeukemia
Kb	Kilo base
LNA	Locked nucleic acids
MiRNA	MicroRNA
mRNA	Messenger RNA
ng	Nanograms
Pre-miRNAs	Precurssor microRNAs

LIST OF ABBREVIATIONS (CONT.)

Pri-miRNAs	Primary microRNAs
PTGS	Post-Transcriptional Gene Silencing
RISC	RNA-Induced Silencing Complex
RNA	Ribo Nucleic Acid
RNAi	RNA interference
RT	Reverse Transcription
RT-PCR	Real Time-Polymerase Chain Reaction
SAGE	Serial analysis of gene expression
SiRNA	Small Interfering RNA
TBE	Tris-Borate-EDTA
T _m	Melting temperature

CHAPTER 1

INTRODUCTION AND BACKGROUND

1.1 Gene Expression and Regulation

Gene expression is a highly complex and well controlled process. For a gene to be stably expressed, the information in double helical DNA is converted into an intermediate form called messenger RNA (mRNA) by the process of transcription. This single-stranded mRNA is then transported out of the nucleus into the cytoplasm and translated into a polypeptide chain. The base sequence in the DNA template and then in mRNA dictates the structure of the final protein product. Stable gene expression is required for normal physiology during development and throughout the entire lifespan of a particular cell. Derailment of any one of these processes can ultimately lead to altered physiology and disease.

Gene expression is controlled at various stages: transcriptional, post transcriptional, translational, and post translational. Transcriptional regulation is the most common and important level because it is the first step in gene expression. A subsequent point at which gene expression is regulated is at the post transcriptional level and can occur by RNA interference or RNAi. This process is known by different names such as post transcriptional gene silencing or PTGS in plants, quelling in fungi, and RNA silencing. RNA interference is mediated by small RNA species such as small interfering RNAs (siRNAs) and the more recently discovered miRNAs. The Nobel Prize for Physiology or Medicine in 2006 was awarded to Andrew Fire and Craig Mello for recognizing RNAi in *Caenorhabditis elegans* as a response of the nematode to exogenously introduced, long double-stranded RNA (dsRNA) [1]. RNAi operates in almost all eukaryotic cells including parasites, insects, protozoa, mouse, and human cells but PTGS was first observed in plants. RNAi was observed serendipitously by Jorgensen's laboratory when

trying to over-express the chalcone synthase (*chsA*) gene that produced purple color of the petals [2]. Homology-dependent gene silencing in fungal systems was reported in *Neurospora crassa* while attempting to increase the production of an orange pigment. Albino phenotypes were produced as a result of quelling when the wild type *all*⁺ gene was transformed with a plasmid construct containing the coding sequence of the *all* gene [3]. RNAi was also observed in virus-infected plants. Plants can be made virus resistant by inoculation with a mild viral strain closely related to a virulent one. The mRNA from the resistant plant assumed a dsRNA conformation and triggered a sequence-specific degradation of homologous cRNA sequences in the cytoplasm [4]. However, it was not until Fire et al [1] demonstrated the biochemical nature of dsRNA-mediated gene silencing by introducing dsRNA directly into the body of *C. elegans* that the process of PTGS was widely accepted.

The siRNA and miRNA maturation pathways are quite similar but it is worthwhile to note the distinctions between them. Mature miRNAs are single stranded and have imperfect complementarity with the cognate mRNA sequence and are derived endogenously. On the contrary, siRNA is most commonly a response to an exogenous RNA. These exogenous RNAs are then converted into short 20-22 nucleotide RNA molecules called siRNAs. The siRNAs then guide degradation of the target mRNA. The siRNAs require a perfect match with the corresponding mRNA sequence to induce silencing.

MiRNAs are a family of short, non-coding, evolutionarily conserved, and endogenous 21-25 nucleotide-long gene regulators that negatively regulate gene expression at the post-transcriptional level [5]. MiRNAs regulate gene expression in two different ways [6]. In the first mechanism which is found in both plants and animals, miRNAs are perfectly complementary to the target mRNA sequence resulting in mRNA cleavage. In the second mechanism, found mainly

in animals, the miRNAs bind to imperfectly complementary sites and block translation by binding to 3'-untranslated regions of their target mRNA. Since the discovery of *lin-4* and *let-7* miRNAs, many workers have aimed at identifying novel miRNAs. This generated the need to avoid redundant identities and provide general access of miRNA genes and their sequences to all investigators [7]. The miRNA registry at the Sanger Institute:

<http://microrna.sanger.ac.uk/registry/> serves these two purposes. First, it establishes nomenclature of the miRNAs to avoid accidental overlap of the gene names. The miRNAs are given a numerical identification based on sequence similarity. Secondly, it provides a comprehensive and open access to the miRNA sequence database. There are 9539 miRNA entries in the miRBase sequence database as of the March 2009 release 13.0.

1.2 A Brief History of miRNA Discovery

MiRNAs were first discovered as gene regulators when genetic screens were performed in the nematode worm *Caenorhabditis elegans* for genes that function in developmental timing during larval development [8]. The founding member of the miRNA gene family, *lin-4*, repressed the expression of LIN-14 protein. This was noted when *lin-4* mutants expressed inappropriate developmental fates and displayed reiterations of early developmental fates [9, 10]. The expression level of *lin-14* is exceptionally high in *lin-4* mutant animals. The *lin-4* transcripts bind with partial complementarity to the 3'-untranslated regions (3'-UTRs) of the *lin-14* transcript and thereby repress its expression. The second RNA discovered to have regulatory functions was *let-7* [11]. It is a heterochronic gene that aids in the temporal regulation of developmental timing. The *let-7* ~22 nucleotide transcripts contain regions complementary to the 3'-UTRs of *lin-14*, *lin-28*, *lin-41*, *lin-42*, and *daf-12*. Loss of the *let-7* gene leads to reiteration of early stage larval development that often results in rupture at their midsection. Conversely, over

expression of the let-7 gene causes an early appearance of adult fates during larval stages. Bantam RNA and miR-14 function in cell death and miR-14 also functions in fat storage in *Drosophila melanogaster* [12]. MiR-181 and miR-375 regulate hematopoiesis and insulin secretion in *Mus musculus* [13, 14] and lsy-6 and miR-273 control neuronal patterning in *C. elegans*[15].

1.3 Biogenesis of miRNA

Primary miRNA (pri-miRNA) transcripts are generated from miRNA genes in the nucleus by RNA polymerase II [16]. The pri-miRNAs are modified at their 5'- and 3'- ends by capping and polyadenylation. The pri-miRNAs contain a stem-loop structure that is imperfectly base-paired. The pri-miRNAs are processed by an RNase III enzyme named Drosha using a cofactor named Pasha to generate a 70 nucleotide long precursor miRNA (pre-miRNA) [16]. In humans, the pri-miRNAs undergo processing by Drosha and its double-stranded RNA-binding protein DGCR8 (DiGeorge syndrome Critical Region 8) [6]. The pre-miRNA is then transported to the cytoplasm by RAN-GTP and exportin-5. Exportin-5 is a member of the nucleocytoplasmic transport proteins named karyopherins and RAN is a GTPase that is active only when bound by GTP [17, 18]. Once in the cytoplasm, the pre-miRNAs are processed by another enzyme, Dicer, to ~22 nucleotide miRNA-miRNA* duplexes. These duplexes are bound by the RNA-induced silencing (RISC) complex containing argonaute proteins. The RISC retains the mature single-stranded miRNA that binds to the complementary mRNA target and thereby represses target gene expression [19].

1.4 Relevance of miRNAs to Physiology and Disease

Before the discovery that miRNAs play an important role in the regulation of gene expression, it was largely believed that most of the genome was silent and not translated into

proteins. In other words, the non coding regions of the genome were considered “junk” DNA. But, it is now clear that miRNAs play wide-ranging roles in silencing their specific target mRNAs. By regulating various pathways, miRNAs contribute greatly to normal physiology and development as well as pathology. This is underscored by an impressive list of diseases associated with abnormal miRNA expression. Increasing evidence suggests that altered miRNA expression is associated with an array of pathological conditions and age-related disorders including cardiovascular diseases, neurological disorders, immune functions, and a number of cancers.

1.4.1 Age- Related Diseases

Accumulating evidence indicates the role of altered miRNA expression in a range of age-related diseases. This mainly results from decreased control of cell signaling that occurs during mid-life for important physiologic processes like the cell cycle, DNA repair mechanisms, apoptosis, and responses to oxidative free radicals. Currently, there is little knowledge of how miRNAs contribute to aging. It is proven that aging involves changes in the expression of protein-coding genes, especially some transcription factors [20]. Knockout of Dicer in mice demonstrated that this multi-subunit protein is involved in mammalian development. Dicer mutants displayed a phenotype of gestational lethality. The same group also found that dicer-deficient mice exhibit abnormal blood vessel development, thereby showing that dicer is required for angiogenesis [21]. Williams et al [22] used semi quantitative RT-PCR to assess the differential expression of miRNAs in the post-natal vs. adult mouse lung. They found that expression of a group of 14 miRNAs including miR-154; miR-323, miR-335; miR-337, and miR-370 were more than 20-fold up-regulated in neonatal lungs compared to adult lungs. On the contrary, expression of miR-29a, miR-29b, miR-29c, miR-51, and miR-52 were 50-fold up-

regulated in adult lung compared to neonatal lung. The same group conducted miRNA profiling using RT-PCR array to determine if alteration of miRNA expression occurs during aging. Using 6 month-old adult mice and 18 month-old aged mice, results contrasted with those from their previous study in developing lung tissue. They found no significant alterations in miRNA expression in aged lung compared to normal adult lung [23]. In *C. elegans*, loss of lin-4 decreased life span and led to tissue aging while over expression of lin-4 extended life span [24]. These studies implicate specific miRNAs in developmental timing and in the regulation of life span.

1.4.2 Cardiac Development and Cardiac Excitability

Normal cardiac development requires coordinated expression of a large number of proteins. Recent evidence suggests that a number of miRNAs including miR-1, miR-133, and miR-208 are involved in the growth and development of cardiac muscles. Alterations in embryonic cardiac development can lead to severe consequences. Chen et al [25] produced a conditional knockout of Dicer in mice and observed a drastic reduction in the levels of mature miRNAs. Dicer-deficient mice exhibited aberrant expression of cardiac contractile proteins and reduced cardiac functions. These mice rapidly progressed to a dilated cardiomyopathy, heart failure, and post-natal death.

In addition to normal heart development, miRNAs have significant roles in pathological conditions of the heart. Cardiac cells are highly prone to hypertrophy in response to injury and stress. This hypertrophic growth, though initially an adaptive response to stress that involves increased cell size, enhanced protein synthesis, and reactivation of fetal genes, ultimately leads to cardiac failure and death. Roonji et al [26] induced cardiac stress in mice by different methods including thoracic aortic banding (TAB) and injection of activated calcineurin A (CnA). TAB-

exposed mice showed an up regulation of 27 miRNAs and CnA-injected mice showed an up-regulation of 33 miRNAs. MiRNA expression is also aberrant in failing human hearts. Northern blot analysis of miRNAs in the idiopathic end-stage failing human heart showed an up regulation of miR-24, miR-125b, miR-195, miR-199a, and miR-214

1.4.3 MiRNAs in Brain Development and Diseases

Numerous studies describe the role of miRNAs in neuronal development. miRNAs are richly expressed in the adult brain and function in the maintenance of mature neural traits like membrane electrical properties, responses to environment inputs, and synaptic plasticity [27]. Development of the central nervous system is a highly coordinated process involving up regulation of neuronal genes and down-regulation of non-neuronal genes. MiR-124 is abundant in the brain and functions in the suppression of anti-neuronal genes. Small C-terminal domain phosphatase 1 (SCP-1) is an important anti-neuronal factor expressed in non-neuronal tissues. The 3'UTR of SCP-1 is a direct target of miR-124 [28]. In situ hybridization using LNA (Locked Nucleic Acids) antisense oligonucleotide against miR-124 in developing mouse and chick spinal cord demonstrated the up-regulation of miR-124 in differentiating neuronal progenitor cells in dorsal root ganglion and lateral neuronal domain of the developing spinal cord. They also found a concomitant decrease in the expression of SCP-1 in the dorsal root ganglion and lateral domain of the spinal cord. This antagonistic expression of miR-124 and SCP-1 suggests that miR-124 suppresses the expression of SCP-1 in the developing CNS, thereby promoting neuronal development.

MiRNAs are also involved in the pathogenesis of neurodegenerative disorders like Alzheimer's disease and Parkinson's disease. Alzheimer's disease results from accumulation of amyloid beta plaques (A β) in the brain. Though the molecular mechanisms of A β formation are

not completely known, decreased clearance of A β is considered one of the causes. MiRNA profiling among brain samples from Alzheimer's disease patients revealed that several miRNAs are involved in the control of BACE1 or β -secretase, the rate-limiting enzyme for formation of A β . Expression of the miR-29a/b-1 cluster was significantly decreased in AD patients with abnormally high BACE1 expression [29].

Parkinson's disease is the second most prevalent age-associated neurodegenerative disorder and is characterized by loss of mid-brain dopaminergic neurons (DN). Kim et al [30] established that Dicer is important for the differentiation of DN. Deletion of dicer using Cre-recombinase during the initial stages of DN differentiation led to the complete loss of DN. Further comparison studies were conducted between a normal adult mouse brain and a brain depleted of mid-brain DN. Expression profiling indicated that one of the precursor miRNAs, miR-133b, was highly enriched in the mid-brain and absent in the brain depleted of DN. The brain samples of Parkinson's patients also lacked miR-133a expression that eventually led to loss of DN control and function.

1.4.4 MiRNAs in Inflammation and the Immune System

The discovery of miRNAs and their involvement in various physiological processes initiated investigations of their role in fine tuning the immune system and inflammation. Investigations in this direction revealed the expression profiles of many miRNAs in hematopoietic tissues and immune-related cells [31]. Involvement of miRNAs in the fine tuning of innate immune responses has been reviewed [32]. In addition to their role in hematopoiesis, miRNAs are also candidates in the inflammatory responses associated with many diseases like psoriasis [33], asthma [34], rheumatoid arthritis [35], and vascular inflammation [36]. Deletion studies established the prominent role of miRNAs in regulation of the immune response.

Deletion of miR-144, miR-181, and miR-223 led to impaired T- cell and B-cell differentiation in the germinal center and reduced antibody and cytokine production [37]. More research into the roles played by miRNAs in immune system function and diseases will provide greater understanding of the processes involved and will help in the development of treatments for many inflammatory diseases.

1.4.5 MiRNA Expression in Endometriosis

Real-time PCR profiling studies of miRNA expression in the endometrium of women with and without endometriosis reported higher expression of miR-23b, miR-23a, miR-17-5p, and miR-542-3p in endometriosis compared to normal endometrium [38]. The expression of genes like aromatase (CYP19A1), steroidogenic acute regulatory protein (StAR), and cyclooxygenase-2 (COX-2) were inversely correlated with over expression of those miRNAs. StAR functions as a rate-limiting factor in steroid synthesis, CYP19A1 is involved in the conversion of testosterone to 17β -estradiol, and COX-2 is involved in the conversion of arachidonate to prostaglandin E2 and also influences the expression of CYP19A1 and StAR. The same study also confirmed differential expression of those miRNAs following treatment of endometrial stromal cells (ESCs) and glandular epithelial cells (GECs) with 17β -estradiol and medroxyprogesterone and their antagonists ICI-182780 and RU-486, respectively. As such, this study is highly significant because it can also be extended to the role played by some of those miRNAs in hormone-dependent cancers.

Uterine epithelium undergoes periodic degenerative and reparative processes in response to steroidal hormones produced by the ovary. The secretion of many of these hormones is influenced by miRNAs. The miRNAs involved in silencing genes involved in various endometrial activities include miR-21, miR-20a, miR-181a, miR-18a, miR-206, and miR-142-

5p. The genes that these miRNAs target include those coding for transforming growth factor- β (TGF- β), estrogen receptors (ERs), progesterone receptors (PRs), and aromatase. Many processes like cell-cycle progression, apoptosis, differentiation and regeneration, inflammation, and immune responses during the menstrual cycle are regulated by miRNAs [39].

Under endocrine control, the adult female reproductive tract (uterus, oviduct, and ovary) undergoes dramatic cyclical changes. These changes require the regulated expression of genes involved in differentiation, proliferation, cell cycle progression, and apoptosis. As mentioned previously, the co-ordinated expression of genes involved in these processes is regulated by miRNAs. In addition to its involvement in the normal development of lungs, limbs, and muscles, the ribonuclease enzyme dicer, which is involved in the biogenesis of miRNA, also plays a major role in development of the female reproductive system. Conditional deletion of Dicer 1 in mice produced infertile females and the uterine horns in Dicer 1 knockout mice were shorter compared to control uteri [40]. In addition to the gross morphological changes observed in the uterus of the Dicer1 knockout mice, their oviducts were fragile and their ovarian weights were reduced.

1.5 MiRNAs and Cancer

Cancer is a manifestation of uncontrolled cell growth, proliferation, and spread to other healthy tissues by the process of metastasis. Cancer is a genetic and epigenetic disease arising from accumulated mutations that activate proto-oncogenes and inactivate tumor suppressor genes [41]. There are intricate mechanisms by which cells normally regulate the processes of cell division, differentiation, and death during early development and at maturity. This synchronization is achieved by fine tuning gene expression and by switching gene expression on and/or off at different stages.

Evidence from various miRNA studies indicate that they play significant roles in the development of malignancies. Screenings for miRNAs indicate that their genes are located at fragile sites and at genomic regions involved in cancers [42]. The expression of specific miRNA genes is both up-regulated and down-regulated in many cancers. Over accumulation of miRNAs that target mRNAs coding for tumor suppressor genes result in less protein product and subsequent loss of protection by the tumor suppressor. On the other hand, loss of miRNAs that target proto-oncogenes leads to the excessive accumulation of oncogenic protein products [43]. Primary evidence for miRNA dysregulation in the pathogenesis of cancer was presented by Calin et al in human chronic lymphocytic leukemia (hCLL) [44]. The miR-15a and miR-16a miRNA genes are located at the chromosome locus 13q14 and were either absent or down-regulated in most cases of chronic lymphocytic leukemia. Cimmino et al [45] later showed that miR-15 and miR-16 target the antiapoptotic protein BCL2. So, their loss/inhibition leads to absence of apoptosis and the pathogenesis of hCLL. Expression of the miRNAs miR-125b, miR-145, miR-21, and miR-155 was deregulated in human breast cancer cells and correlated to the expression of hormone receptors, tumor stage, vascular invasion, and metastasis [46]. The accumulation of BIC RNA, a polyadenylated and non-coding RNA, was described as a prognostic and diagnostic signal in DLBCL. The bic locus is recognized as the insertion site for proviral DNA in avian leukosis virus-induced lymphomas [47]. Activation of the BIC gene accelerates the pathogenesis of leukemias and lymphomas by up-regulating the c-MYC oncogene. The cytoplasmic copy numbers of miR-155 miRNA which can be processed from BIC RNA is high in DLBCL compared to normal B-cells [48]. MicroRNA profiling using RT-PCR showed that three miRNA species (miR-221, miR-376a, and miR-301) were differentially expressed in pancreatic adenocarcinoma [49]. Those findings demonstrate that miRNA profiling

is an important prognostic and diagnostic tool in the treatment of many malignancies. Very recently, miRNAs were shown to control the tumor suppressor p53, also known as guardian of the genome. P53 is activated in the wake of DNA damage occurring during cell division. Expression of the miR-34 family that consists of three members in the vertebrate genome (miR-34a, b, and c) is induced by DNA damage and induces apoptosis in neuroblastoma cells [50]. The biogenesis of miRNA involves complex nucleotide processing and employs diverse protein machinery. During maturation, the Drosha processing step regulates the concentration of miRNA transcripts. Discrepancies in this step have severe impacts on the expression of miRNA genes both in normal development and in cancer [51]. Reduced expression of dicer also correlates with a poor prognosis for lung cancer associated with poor post-operative survival and a poor tumor differentiation state [52].

1.6 MiRNA Profiling Classifies Cancer Types

MiRNA profiling is a new clinical tool in the classification, prognosis, and diagnosis of cancer [53]. MiRNA profiling has been used to establish a correct diagnosis in cases of metastatic cancers from unknown primary sites and for tumor types that cannot be determined on the basis of biopsy samples. Poorly differentiated tumors have a lower miRNA expression profile compared to well-differentiated tumors. Several techniques have been used for miRNA expression profiling including oligonucleotide array, bead-based flow cytometry, RT-PCR, Northern blotting, SAGE (Serial Analysis of Gene Expression), and microarray. Liu et al [54] described a highly reproducible technique using oligonucleotide microchip-based profiling for tissue-specific microRNA expression that was confirmed by Northern blots and RT-PCR. They used a bead-based flow cytometric method to screen around 217 miRNAs from 334 samples and thereby generated important and informative clues regarding the developmental lineage and the

differentiated state of solid tumors. This technique is much more specific and superior to glass-based hybridization techniques. Another new and efficient method using locked nucleic acid-based Northern blot analysis was explained by Valoczi et al [55]. By screening human colorectal cancer cells, many new miRNAs and known mature miRNA forms were identified using serial analysis of gene expression for miRNAs (miRAGE) by Cummins et al [56] at the Sidney Kimmel Comprehensive Cancer Center.

MiRNAs are differentially expressed in cancer cells and normal cells. A microarray analysis using 540 cancer samples that included the six most common human solid tumors and 177 normal controls found that cancer cells and normal tissue cells exhibit considerable differences in miRNA expression profiles [57]. Extensive research on miRNA deregulation was conducted on many human cancers. Ciafre et al used microarray for global expression profiling of glioblastoma multiforme, the most malignant of the primary brain tumors, and they found that miRNA miR-221 was strongly up-regulated in glioblastoma while miR-181a and miR-181c were down-regulated [58]. Expression profiling of miRNAs in normal pancreas, pancreatic acinar tumors, and pancreatic endocrine tumors determined that miR-103 and miR-107 were up-regulated and expression of miR-155 was lacking in pancreatic acinar tumors compared to the normal pancreas [57]. Murakami et al [59] reported differential expression of miRNAs in hepatocellular carcinoma, chronic hepatitis, and liver cirrhosis samples. Microarray profiling of malignant and non-malignant cholangiocytes showed a decreased expression of many miRNAs in the malignant cells. To identify and recognize specific miRNAs involved in tumor cell growth and response to chemotherapy, Meng et al reported an altered expression of miRNAs following treatment with the apoptosis-inducing agent, gemcitabine. [60]. Different degrees of miRNA expression are found in different cancers. For instance, He et al showed an 11 to 19-fold up-

regulation of miR146, miR-221, and miR-222 in human papillary thyroid carcinoma (PTC) compared to normal thyroid tissue [61]. However, other studies showed a less dramatic difference in miRNA gene expression. Using microarray-based global gene expression profiling, Wang et al [62], showed that five miRNAs (let-7 family, miR-21, miR-23b, miR-29b and miR-197) were deregulated in uterine leiomyomas.

1.7 MiR-21: A miRNA Up-Regulated in Cancers

Large-scale profiling experiments show that miR-21, which is perfectly conserved in mammals, is up regulated in many cancers. Volinia et al [57] profiled 540 human samples representing 363 solid cancers and 177 normal samples and confirmed that miR-21 expression is up regulated in all types of analyzed cancers including the breast, lung, pancreas, colon, and stomach. Using TaqMan quantitative real-time PCR, Zhang et al [63] found that miR-21 expression is up regulated in human gastric cancer tissues and cell lines as well as *H. pylori*-infected gastric mucosa. They also conducted forced expression and knock-down analysis in the AGS gastric epithelial cells, a human gastric cancer cell line, and found that forced expression of miR-21 led to increased cell proliferation and invasion, while knock down of miR-21 significantly decreased cell proliferation and cell invasion as well as enhanced apoptosis [63]. Over expression of miR-21 was also demonstrated in hepatocellular carcinoma using miRNA microarray profiling studies and was linked to suppressed expression of phosphatase and tensin homolog (PTEN), a tumor suppressor. Enhanced expression of miR-21 increased tumor cell invasion, proliferation, and migration [64]. Additionally, over expression of miR-21 occurs in ovarian cancer [65], cervical cancer [66], leukemia [67, 68], and B-cell and Hodgkin lymphoma [69]. These observations of miR-21 over expression in many cancers, especially in more

malignant and advanced tumors and its role as an important regulatory miRNA, suggest that miR-21 expression can be used as a diagnostic and prognostic marker in cancer [70].

1.8 Inhibition of MiRNAs as a New Therapeutic Strategy

The role of miRNAs as repressors of translation provides a new direction in specifically inhibiting a gene or clusters of genes. Synthetic analogs of these non-coding RNAs called “antagomirs” or anti-miRNA oligonucleotides (AMOs) can specifically suppress the expression of a miRNA of interest [71]. Different types of modified AMOs will silence specific miRNA targets. Three major types are oligonucleotides modified at the 2'-OH residues of ribose by 2'-O-methyl, (2'-OMe), 2'-O-methoxyethyl (2'-MOE), and locked nucleic acids (LNA) [72]. These modifications prevent attack of the oligonucleotides by serum and cellular nucleases. Other trial modifications include phosphorothioate backbone and cholesteryl esters. Addition of cholesterol to the 3' end of oligonucleotides improves pharmacokinetic properties such as half-life in serum and cellular uptake [71]. In the first trial using antagomirs to specifically silence miRNA expression in mice, Krutzfeldt et al [73] used a single intra venous injection of cholesterol-conjugated, single-stranded RNA molecules complementary to the mature miRNA to suppress the expression of miR-122 in liver, lungs, intestine, heart, skin, and bone marrow. The first example of using AMOs as a therapeutic strategy was provided by Esau et al, who inhibited miR-122 expression leading to reduced plasma cholesterol and reduced hepatic fatty acid and cholesterol synthesis [74]. This study also proved the potential role of miR-122 in cholesterol and fatty acid metabolism. More understanding of specific miRNA signatures in human diseases will eventually give way to targeted therapy, better diagnosis and prognosis, and the identification of new therapeutic targets.

1.9 Endocrine Disruption and DES Exposure

Chemicals that mimic natural hormones can act as endocrine disruptors. Neonatal and prenatal exposure to these chemicals can impair normal development of the reproductive tract and its adult function. DES is considered a potent xenoestrogen and endocrine disruptor. Synthesized in 1938, DES is an orally active synthetic estrogen that was prescribed to women in the mistaken belief that it would prevent miscarriages in high-risk and normal pregnancies. More than 4 million Americans may have been exposed in utero to this teratogen [75]. The first clinical evidence of vaginal clear cell adenocarcinoma in a group of young women exposed in utero to DES was reported by Herbst et al [76]. This observation triggered extensive epidemiological and experimental investigation of the long-term consequences of perinatal DES exposure. Using global gene expression profiles and gene knock-down mouse models, Huang et al [77] proved that neonatal DES treatment altered genetic pathways of uterine epithelial differentiation. Other studies also implicate epigenetic alterations in DES-induced carcinogenesis. Studies on lactoferrin gene expression in perinatally DES-treated mice showed that altered gene methylation is an early event in DES-induced uterine cancer [78]. Reproductive tract abnormalities ranging from cryptorchidism, testicular tumors, involution of accessory sex organs, and epididymal cysts occur in adult male hamsters treated with DES on the day of birth [79]. Spermatogenesis, the process of sperm maturation, was disrupted along with accumulation of multinucleated epididymal epithelial cells and abnormal seminal vesicle morphology. Testicular seminoma and testicular tumors are also reported in mice exposed to DES in utero [79]. Interstitial cell tumors were observed in the adult male offspring of mice treated with 100µg/kg body weight of DES through 9-16 days of gestation. An overall incidence of 8% for

testicular tumors was reported in the prenatally treated mice. Rete testes lesions that resemble adenocarcinoma were reported in prenatally DES-treated male mice [80].

Here we report the results of a pilot project to test if altered miRNA expression is involved in neonatal DES-induced uterine cancer in our hamster experimental system. Previous studies in this system [41, 42] demonstrated that neonatal DES exposure induced an early and permanent developmental change in the prepubertal uterus (initiation stage). This initiation-stage process then leads to an abnormal response of the adult uterus to natural endogenous estrogen synthesized by the adult ovary (promotion stage), ultimately leading to the development of endometrial adenocarcinoma. For the initiation stage, total RNA was isolated from uteri harvested from 5-day old hamsters. The rationale being that the neonatally DES-exposed uteri exhibit an abnormal uterotrophic response that peaks at that time. For the promotion stage, total RNA was isolated from uteri harvested from adult (2-month old) hamsters that were ovariectomized prepubertally (day 21) and then chronically stimulated with estrogen. The rationale being that neonatally DES-exposed animals at this age and under this endocrine environment exhibit distinct precancerous characteristics including hyperplastic lesions and gross histomorphological changes [41].

1.10 Hypothesis and Specific Aims of the study

The working hypothesis tested in this research was: Alterations in miRNA expression are part of the process by which neonatal DES exposure induces estrogen-dependent uterine cancer in the hamster. The strategy used to test this hypothesis is as follows:

1. Extract total RNA from control and neonatally DES-exposed hamster uteri at both the initiation and promotion stages of the induced uterine adenocarcinoma phenomenon.

2. Use a micro-array system to screen for altered miRNA expression in both stages of the neonatal DES-induced uterine cancer phenomenon.
3. Validate the miRNAs that had two-fold or more and statistically significant differential expression in the DES-treated uterine samples compared with the control samples using qRT-PCR.

CHAPTER 2

MATERIALS AND METHODS

2.1 Animals

Pregnant adult female Syrian hamsters were purchased from Harlan Sprague Dawley Inc, IN, and maintained in a climate-controlled room with a 14-h light and 10-h dark cycle and at 23-25°C with free access to food and water according to the Wichita State University Institutional Animal Care and Use Committee (IACUC) guidelines.

2.2 Experimental Design

Within 6 hours of birth (day 0), the new-born hamsters were sexed and litter size was adjusted to 8 neonates per litter by eliminating extra males. The adjusted litter received a single inter-scapular, subcutaneous injection of 50µl corn oil either alone (control hamsters, CON) or containing 100µg DES. This DES dose level is equivalent to approximately 33mg/kg body weight. For the initiation stage samples, uteri were harvested from 5-day old intact animals. For the promotion stage samples, uteri were harvested from 2-month old adult animals that were prepubertally ovariectomized (Ovex) on day 21 of life and also received an implant that maintains circulating estradiol (E₂) levels at a high but physiological level (~200 pg/ml serum) in both control and neonatally DES-exposed animals (Ovex+E₂). The animals were anesthetized with 0.075mg/100mg body weight of Nembutal injected intraperitoneally. The Ovex+E₂ animals also received a microchip implant so that each animal can be identified by an alphanumeric number using an electronic chip scanner. All harvested tissues were immediately frozen on dry ice and then stored at -70°C until processing for total RNA isolation.

2.3 Total RNA Isolation

Total RNA from stage-specific frozen uterine tissue was isolated using the Qiagen® miRNeasy® mini kit (Qiagen Sample and Assay Technologies, CA). The Qiagen® miRNeasy® mini kit employs a combination of phenol/guanidine-based lysis of samples and a silica membrane-based purification of total RNA. The kit includes a monophasic solution of phenol and guanidine-based QIAzol lysis reagent that is designed to efficiently remove DNA and proteins as well as inhibit RNases. Close to 25mg of frozen uterine tissue was used and a proportionate quantity of QIAzol lysis reagent was added (700µl/25mg tissue) and homogenized. The tissue weights and the quantity of lysis buffer used are summarized in Tables 1 and 2.

TABLE 1

TISSUE WEIGHTS AND VOLUME OF LYSIS BUFFER ADDED FOR INITIATION STAGE

Samples	I, C1	I, C2	I, C3	I, D1	I, D2	I, D3
Tissue weight (mg)	42.7	41.4	33.7	44.5	45.1	51.6
Lysis buffer (µL)	1,196	1,160	944	1,246	1,262	1,444

TABLE 2

TISSUE WEIGHTS AND VOLUME OF LYSIS BUFFER ADDED FOR PROMOTION STAGE

Samples	P, C1	P, C2	P, C3	P, C4	P, D1	P, D2	P, D3	P, D4
Tissue weight (mg)	26	27	30	35	28	28	29	29
Lysis buffer (µL)	728	746	840	980	784	784	812	812

The homogenate was separated into an aqueous and organic phase. The RNA partitions into the upper aqueous phase whereas the DNA and proteins partition into the interphase and the lower organic phase, respectively. The isolated upper phase received 525µl of 100% ethanol to provide an appropriate binding condition for RNA molecules including small RNAs from 18 nucleotides upwards. The samples were then applied to the RNeasy mini spin column and treated

with buffers RWT and RPE to wash away phenol and other contaminants. The RNA was then eluted in RNase-free water. Adequate care was taken at all steps to prevent degradation of RNA by RNases. The extracted total RNA was then run on a 1% agarose gel and also sent for quality control to the microarray facility at The University of Kansas Medical Center (KUMC) for evaluation using the Agilent Bioanalyzer 2100.

2.4 MiRNA Profiling

Our global miRNA expression analysis employed Thermo Scientific Dharmacon RNAi Discovery and Therapeutic services (RDTS). The Thermo Scientific Dharmacon miRNA profiling platform utilizes a two-color, high-density, 8-plex chip comprised of probes that capture all human, mouse, and rat mature miRNAs in the Sanger database. The use of unique, dye-labeled internal reference samples increases the sensitivity and robustness of the expression analysis. High sensitivity in the range of sub-attomole detection limits combined with the requirement for sample input as low as 30ng total RNA confers the Dharmacon miRNA expression analysis with important advantages over other commercially available miRNA profiling technologies.

2.5 Validation of the Profiling Results by Quantitative Real-Time PCR

Real-time PCR (RT-PCR) using the TaqMan[®] microRNA Assays and the Step one Real-time PCR system (Applied Biosystems Inc, Foster City, CA) was employed to validate miRNAs that, according to the profiling data, had two-fold or more and statistically significant differential expression in the DES-treated tissue total RNA samples compared with the control tissue total RNA samples. The TaqMan[®] miRNA Assays are designed to detect and accurately quantify mature miRNAs using step-one real-time PCR machines (Applied Biosystems Inc, Foster City, CA).

The TaqMan miRNA assays employ a looped-primer RT-PCR that can accurately detect mature sequences of miRNAs. Each assay contains a miRNA-specific RT Primer, miRNA-specific forward and reverse primers, and a miRNA-specific TaqMan MGB probe. TaqMan miRNA assays are available for a wide range of species.

The quantification using TaqMan assays consists of two steps:

1. A reverse transcription (RT) step where a cDNA (complementary DNA) is reverse transcribed from total RNA samples using specific miRNA primers in the TaqMan miRNA reverse transcription kit.
2. A PCR step in which PCR products are amplified from the cDNA samples generated in the RT step using the TaqMan miRNA assay and the TaqMan Universal PCR Master Mix.

The TaqMan assays use a MGB probe that contains a reporter dye called FAM dye linked to the 5'-end of the probe, a minor groove binder (MGB) at the 3'-end of the probe which increases the melting temperature (T_m) without increasing probe length, and a non-fluorescent quencher (NFQ) at the 3'-end of the probe. The 5'-nuclease assay process occurs during the PCR amplification step. During PCR amplification, the MGB probe anneals specifically to a complementary sequence between the forward and reverse primers. The proximity of the reporter dye to the quencher dye results in suppression of the reporter fluorescence by Förster-type energy transfer. The two-step TaqMan RT-PCR is pictorially represented in [Figure 1](#).

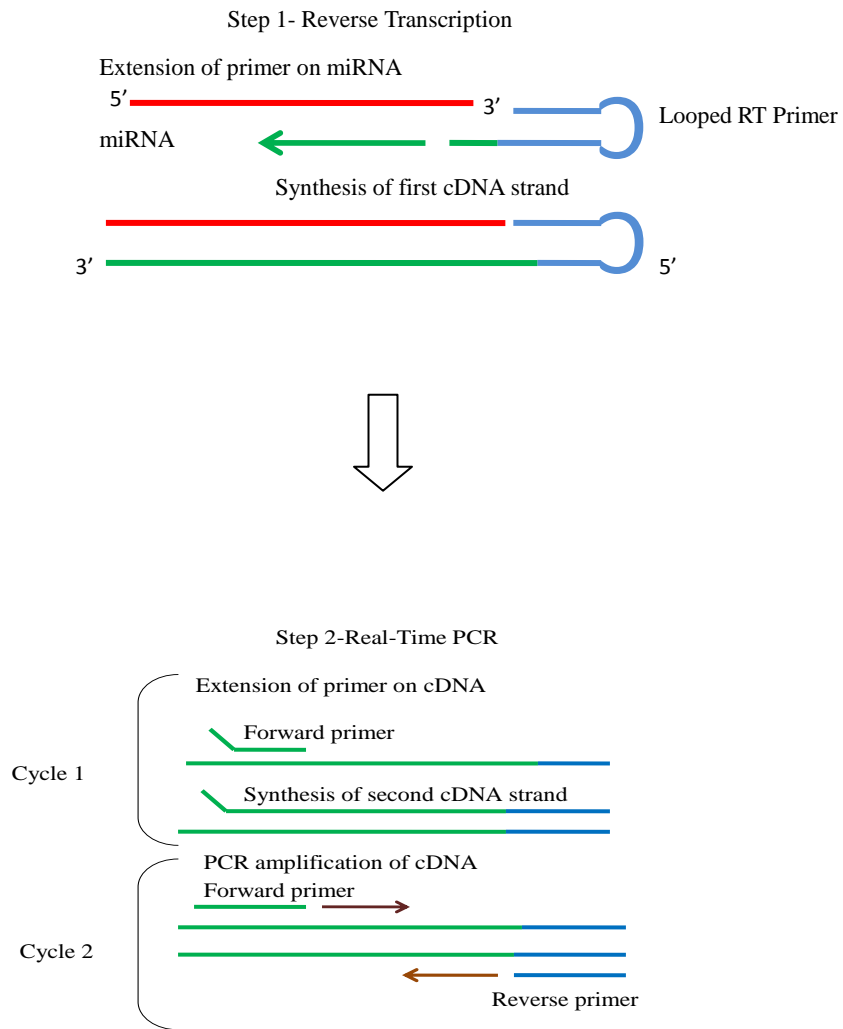


Figure1. Two-Step RT-PCR Assay

As polymerization progresses, the DNA polymerase cleaves probes that are hybridized to the target. This cleavage of the reporter dye from the quencher results in increased fluorescence. This increase in the amount of fluorescence occurs only if the target sequence is complementary to the probe and is amplified during the PCR process. Because of the requirement for exact complementarity, the process does not generate any non-specific amplification.

Each TaqMan assay consists of an RT primer, a TaqMan assay containing pre-formulated forward and reverse primers, a MGB probe, and a reverse transcription kit. For the reverse transcription step, the RT master mix was prepared using the following components: 100mM dNTP mix, Multiscribe Reverse transcriptase, 10X RT buffer, RNase inhibitor. To account for pipetting losses, a 15% excess of all components was used. The detailed list of RT components can also be found in [Table 3](#).

Total RNA samples in triplicate from control and DES-treated groups were diluted to a final concentration of 2.0ng/ μ l. To the sample/master mix mixture, 3.0 μ l of target-specific RT primer was added. The entire RT reactions were stored on ice for 5 minutes and then reverse transcription was performed in a thermal cycler (Eppendorf NA, Westbury, NY) using the settings given in [Table 4](#).

TABLE 3

REVERSE TRANSCRIPTION REACTION COMPONENTS

Component	Master Mix volume/15 μ l Reaction
100mM dNTP's (with dTTP)	0.15
MultiScribe™ reverse Transcriptase 50U/ μ l	1.00
10X Reverse Transcription Buffer	1.50
RNase Inhibitor, 20U/ μ l	0.19
Nuclease-free water	4.16
Total	7.00

TABLE 4

REVERSE TRANSCRIPTION PARAMETERS

Step Type	Time (min)	Temperature (° C)
Hold	30	16
Hold	30	42
Hold	5	85
Hold	∞	4

The cDNA product from the RT step is then used in the PCR amplification step. For this step, a PCR cocktail was prepared for each triplicate set of sample reactions with 12.5% excess of all reagents to account for pipetting losses as given in [Table 5](#).

TABLE 5

REAL-TIME COCKTAIL COMPONENTS

Component	Volume (μl)/ 20- μl Reaction
TaqMan MicroRNA Assay (20X)	1.00
Product from RT reaction	1.33
TaqMan 2X Universal PCR Master Mix, No AmpErase UNG	10.00
Nuclease-free water	7.67

To 48-well optical reaction plates (Applied Biosystems Inc., Foster City, CA), 17.67μl of this master mix was added for each 20μl reaction. Next, 1μl of 20X TaqMan miRNA assay mix and 1.33μl of the RT product were added to the master mix carefully such that the components were placed at the bottom of each well. Then, the PCR reaction plate was sealed with an optical adhesive film and loaded into the StepOne instrument for performance of the real-time PCR following the parameters given in [Table 6](#). StepOne™ software (Applied Biosystems Inc, Foster City, CA) was used to set-up, run, and analyze the real-time PCR

amplification step. The StepOne software supplied with the StepOne Real-time PCR systems allows setting up the reaction plate in simple steps and in a user-friendly manner.

TABLE 6

REAL- TIME PCR PARAMETERS

Step	Amplitaq Gold enzyme activation Hold	PCR cycle (40 cycles)	
		Denature	Anneal/extend
Time	10 min	15 Sec	60 Sec
Temp (° C)	95	95	60

CHAPTER 3

RESULTS

2.6 Total RNA Isolation

The total RNA samples extracted from stage-specific control and DES-treated uterine samples using the procedure discussed above were analyzed spectrophotometrically to assess their quality. Total RNA samples were also extracted from two adjacent pieces of a uterine horn isolated from a normal hamster (NU 1, 2) and used to assess if reproducible quantities of RNA can be prepared from different preps. The spectrophotometric readings of all these RNA samples are listed in Table 7.

TABLE 7

SPECTROPHOTOMETER READINGS FOR TOTAL RNA

Samples	A _{260/280}	A _{260/230}	Total RNA concentration (µg/µl)
Initiation stage			
I, C1	2.07	2.48	0.6887
I, C2	2.04	2.5	0.4129
I, C3	2.02	2.62	0.4793
I, D1	2.07	2.2	1.1248
I, D2	2.01	2.33	0.6046
I, D3	2.05	2.32	1.3258
Promotion stage			
P, C1	2.04	2.49	0.6703
P, C2	2.02	2.34	0.9121
P, C3	2.05	2.37	0.7086
P, C4	2.03	2.42	0.4628
P, D1	2.1	2.34	0.7311
P, D2	2.03	2.22	0.7383
P, D3	2.06	2.25	0.5363
P, D4	2.01	2.26	0.4028
Normal Uterus			
NU 1	2	2.36	0.9127
NU 2	2.05	2.33	1.0435

The samples were further analyzed in a 1% agarose gel in 1X TBE buffer along with 1Kb Riboladder™ (Fisher Scientific, Waltham, MA) as size markers and stained using ethidium bromide, as shown in Figures 2, 3 and 4 for total RNA from normal uterus, initiation stage, and promotion stage, respectively.

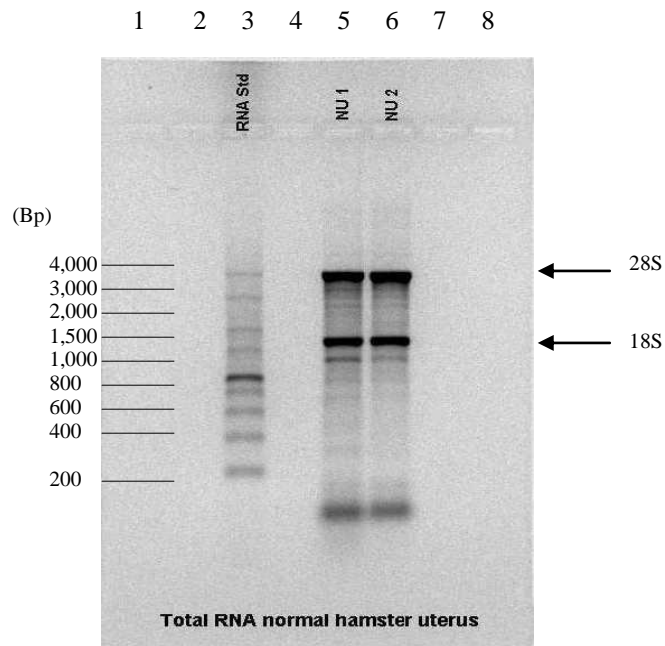


Figure 2. Total RNA (1 μ g) extracted from a normal hamster uterus and run on a 1% agarose gel. Lane 3 represents 1kb RNA ladder and lanes 5 & 6 represent NU1 and NU2 respectively. The numbers in the right margin refer to 28s and 18s rRNA and the numbers in the left margin denote sizes of the RNA standards in base pairs (Bp).

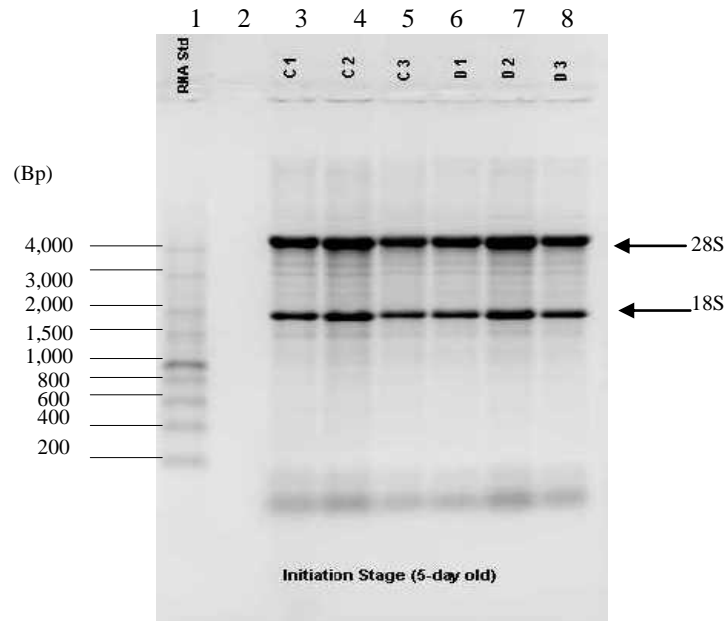


Figure 3. Total RNA (1 μ g) from initiation stage samples analyzed on a 1% agarose gel. Lane 1 represents the 1kb riboladder while lanes 3-5 represent RNA from control uteri and lanes 6-8 represent RNA from DES-exposed uteri. The numbers in the right margin refer to 28s and 18s rRNA and the numbers in the left margin denote sizes of the RNA standards in base pairs (Bp).

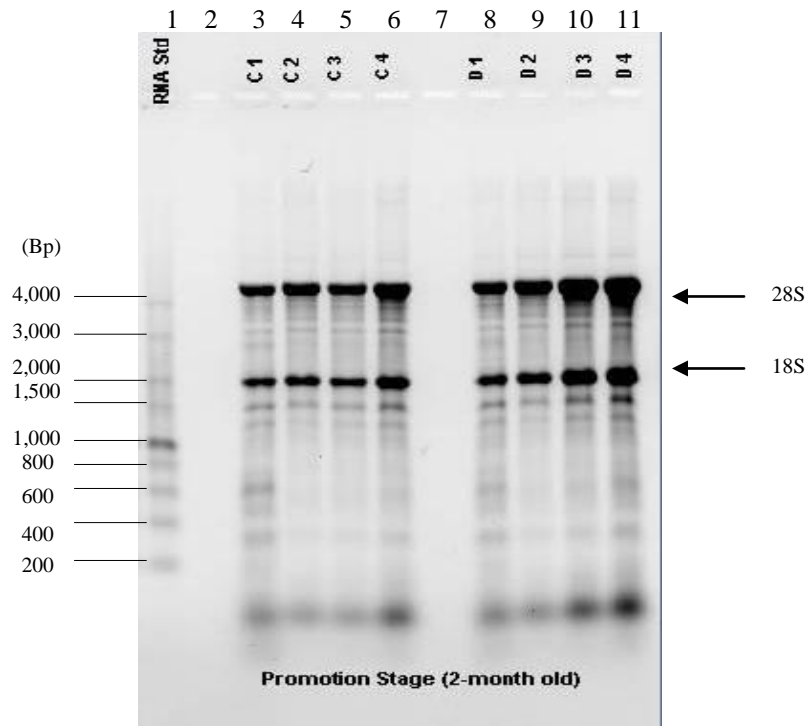


Figure 4. Total RNA (1 μ g) from promotion stage samples analyzed on a 1% agarose gel. Lane 1 represents 1kb riboladder while lanes 3-6 represent RNA samples from control uteri and lanes 8-11 represent RNA from DES-exposed uteri. The numbers in the right margin represents 28s and 18s rRNA and the numbers on the left margin denote sizes of the RNA standards in base pairs (Bp).

2.7 Total RNA Quality Control

Aliquots (5 μ g) of the total RNA samples in triplicate representing both initiation (I) and Promotion (P) stage groups of RNA from Control (C) and neonatally DES-exposed (D) uteri were sent to the University of Kansas Medical Center (KUMC) Microarray Facility for further quality control using an Agilent Bioanalyzer 2100 system (Agilent Technologies, Foster City, CA). To determine if reproducible amounts and quality of total RNA could be prepared, aliquots of the NU 1, 2 samples were also sent for analysis. Due to RNA's high degree of vulnerability to RNases, checking final input sample integrity must be performed before conducting a microarray

experiment. The Agilent Bioanalyzer uses a lab-on-a-chip method to perform capillary electrophoresis and utilizes fluorescent labeling to assess both the quantity and integrity of total RNA. The electropherogram generated by the 2100 Expert software is shown in [Figure 5](#).

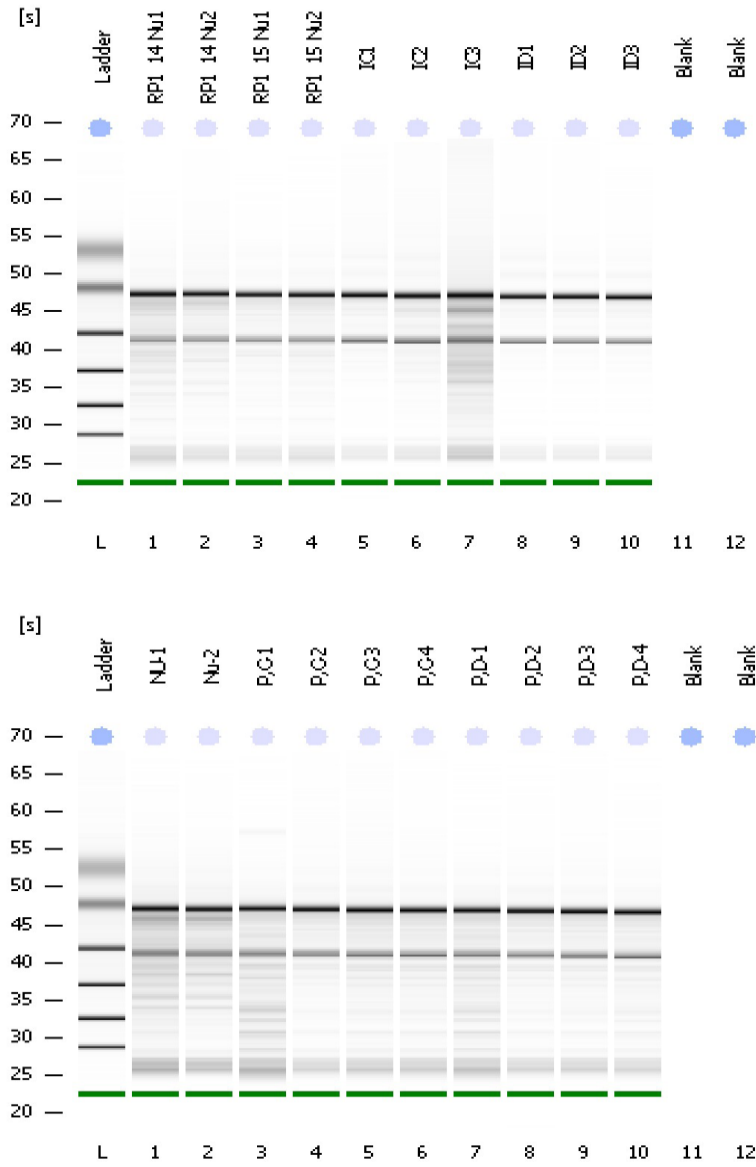


Figure 5. Electropherogram for total RNA samples from NU plus initiation stage (top) and NU plus promotion stage uteri (bottom). [S] denotes the start and end time of peak generation in seconds.

The analysis uses traditional electrophoresis principles and very small sample volumes to generate quality data. The 2100 Expert software generates the RIN (RNA Integrity Number) to estimate RNA quality and also calculates the 28S/18S ribosomal RNA ratios for each total RNA sample. The RIN is a powerful tool to assess RNA quality. For total RNA input samples, the microarray analysis service recommends acceptable RIN numbers of 7-10 and 28S/18S ribosomal RNA ratios of approximately 2.0. The Agilent quality control data for the NU 1, 2 and both the initiation stage and promotion stage RNA samples is summarized in [Figures 6 and 7](#).

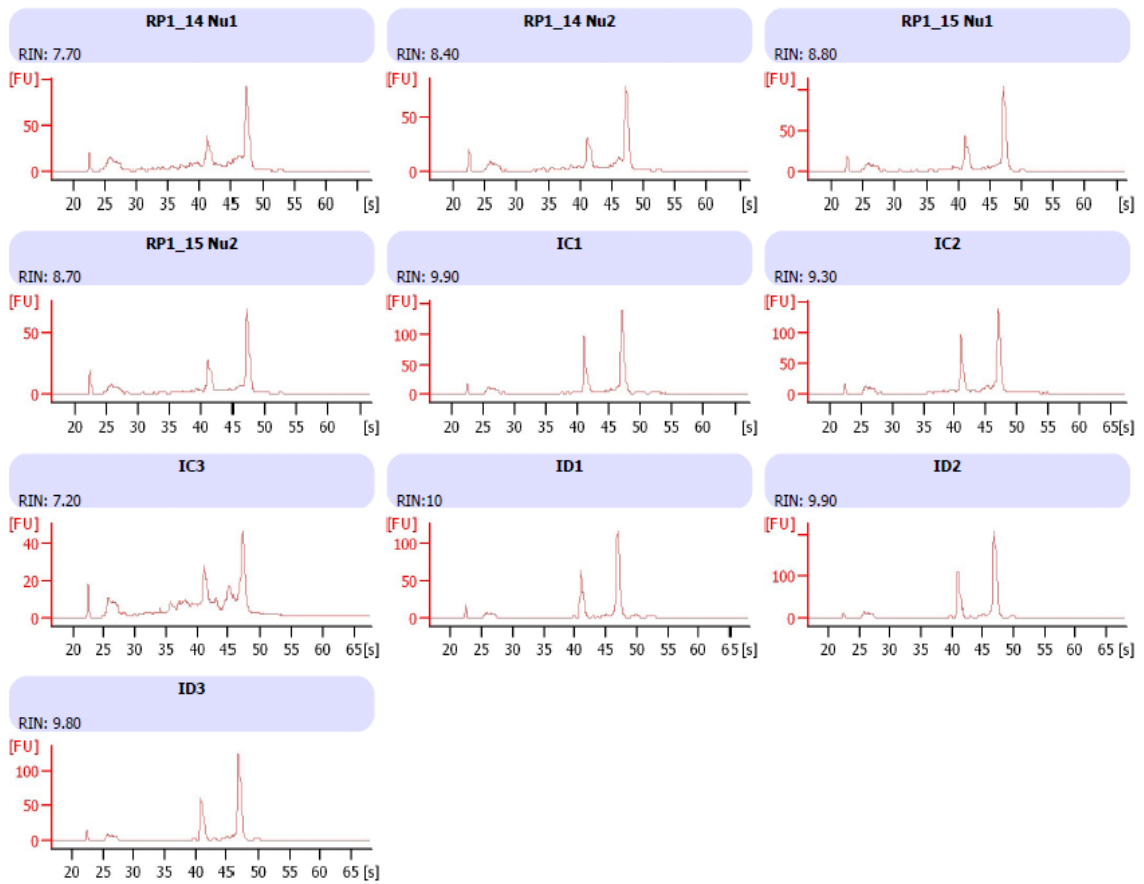


Figure 6. Bioanalyzer 2100 data for NU and initiation stage samples. The X-axis indicates time in seconds and Y-axis indicates fluorescence

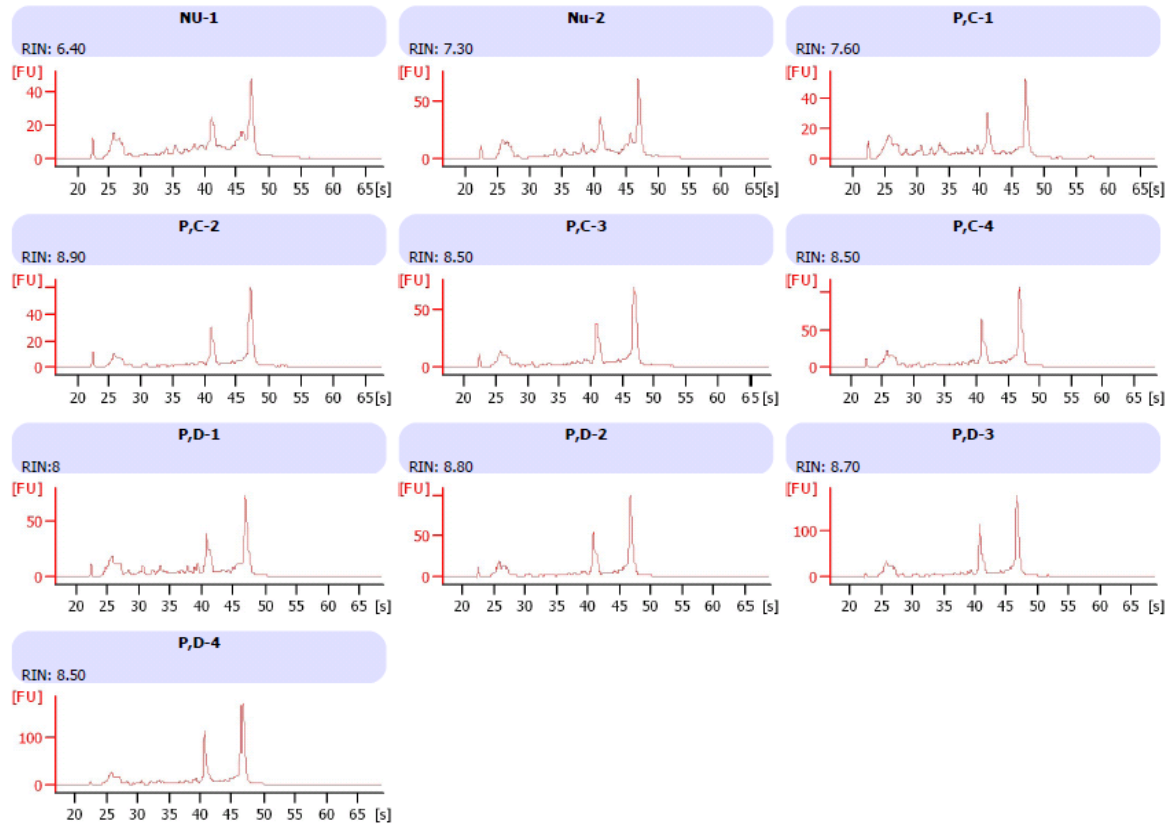


Figure 7. Bioanalyzer 2100 data for NU and promotion stage stage samples. The X-axis indicates time in seconds and Y-axis indicates fluorescence

The RIN numbers and the 28S and 18S ribosomal peak ratios for total RNA samples are summarized in Tables 8 and 9 for the initiation stage and promotion stage groups respectively.

TABLE 8

RIN NUMBER AND rRNA RATIO OF TOTAL RNA SAMPLES FROM THE INITIATION STAGE

Sample	RIN Number	rRNA peak ratio
I, C1	9.9	1.7
I, C2	9.3	1.6
I, C3	7.2	1.8
I, D1	10	1.8
I, D2	9.9	2.0
I, D3	9.8	1.9

TABLE 9

RIN NUMBER AND rRNA RATIO OF TOTAL RNA SAMPLES FROM THE PROMOTION STAGE

Sample	RIN Number	rRNA peak ratio
P, C1	7.6	1.9
P, C2	8.9	2.0
P, C3	8.5	1.9
P, C4	8.5	1.9
P, D1	8.0	2.0
P, D2	8.8	2.0
P, D3	8.7	2.0
P, D4	8.5	1.9

3.3 MiRNA Microarray

Good quality total RNA representing triplicates of control and DES-treated animals were sent to Dharmacon miRNA microarray Services for expression analysis. Two chips each containing eight arrays were used for the study; I-stage samples on one, P-stage samples on the other and NU 1, 2 samples on both. Each array was bar-coded and given an experiment name and factor corresponding to the stage and animal treatment regimen as summarized in Tables 10 and 11.

TABLE 10

CHIP BAR CODES FOR INITIATION STAGE

Chip Barcode	Experiment Name	Factor
251938010078_1_3	I, C-1	IC
251938010078_1_4	I, C-2	IC
251938010078_2_1	I, C-3	IC
251938010078_2_2	I, D-1	ID
251938010078_2_3	I, D-2	ID
251938010078_2_4	I, D-3	ID

TABLE 11

CHIP BAR CODES FOR PROMOTION STAGE

Chip Barcode	Experiment Name	Factor
251938010079_1_3	P, C-2	PC
251938010079_1_4	P, C-3	PC
251938010079_2_1	P, C-4	PC
251938010079_2_2	P, D-2	PD
251938010079_2_3	P, D-3	PD
251938010079_2_4	P, D-4	PD

The data was analyzed in two separate analyses. In the first case, NU samples were included for inter- and intra-array normalization. The assumption was that the relative intensity of NU samples should be: 1) similar both with-in the chip and between the chips, but 2) different from both the control and the DES samples from both stages. First, analysis was done for all eight samples in both the “I” and “P” sets. Relative intensity data was statistically filtered retaining miRNA probes that had p values <0.05. This resulted in 661 miRNA probes in the initiation stage (set “I”) and 644 miRNA probes in the promotion stage (set “P”). This set of miRNAs was inter-array scaled and log (2) transformed. For each set, differential expression analysis was performed using Error-Weighted (EW) ANOVA. For each treatment factor there were 3 factor levels and for one factor level NU, there were only 2 replicates. For this reason, a text book ANOVA could not be performed. As the EW-ANOVA produces more false positive results, a stringent Holm multiple test correction was used which reports a Holm P* value. As each analysis had three treatment levels, the ANOVA was followed by a Sheffe post-hoc test to show differences in miRNA signals in each pair-wise comparison of treatment levels. For identifying miRNA hits that had differential expression, a P*-value of 0.01 was used to identify probes with signals that differ significantly among the three treatment levels. For each treatment level, miRNA probes were chosen with a post-hoc P-value <0.1. The selected hits for each pair

of treatment levels are shown in the scatter plots as represented in [Figures 8 and 9](#). The figures show the selected miRNA hits for pair-wise comparisons of IC vs. ID, IC vs. NU and ID vs. NU. In IC vs. ID, there were 104 probes out of 661 miRNAs that had significant differential expression; in IC vs. NU, 197 probes had significant differential expression; and in ID vs. NU, 200 probes had significant differential expression. In set “I”, a total of 222 miRNA probes had significant differential expression at P*-value <0.01. On the other hand, in set “P”, only 40 miRNA probes had significant differential expression. In PC vs. PD, a total of 16 miRNA probes out of 644 miRNAs had significant differential expression. In PC vs. NU, a total of 33 probes, and in PD vs. NU, a total of 37 probes had significant differential expression, respectively. This subset of probes was used for hierarchical clustering with Z-transformed signals. The Z-transform normalizes the signals for individual miRNA probes so that the mean = 0 and standard deviation = 1 across eight samples. The hierarchical clustering with Z-transformed signals clearly highlights miRNA probes based on differential signals. The hierarchical clustering for the set “I” and set “P” are shown in [Figures 10 and 11](#).

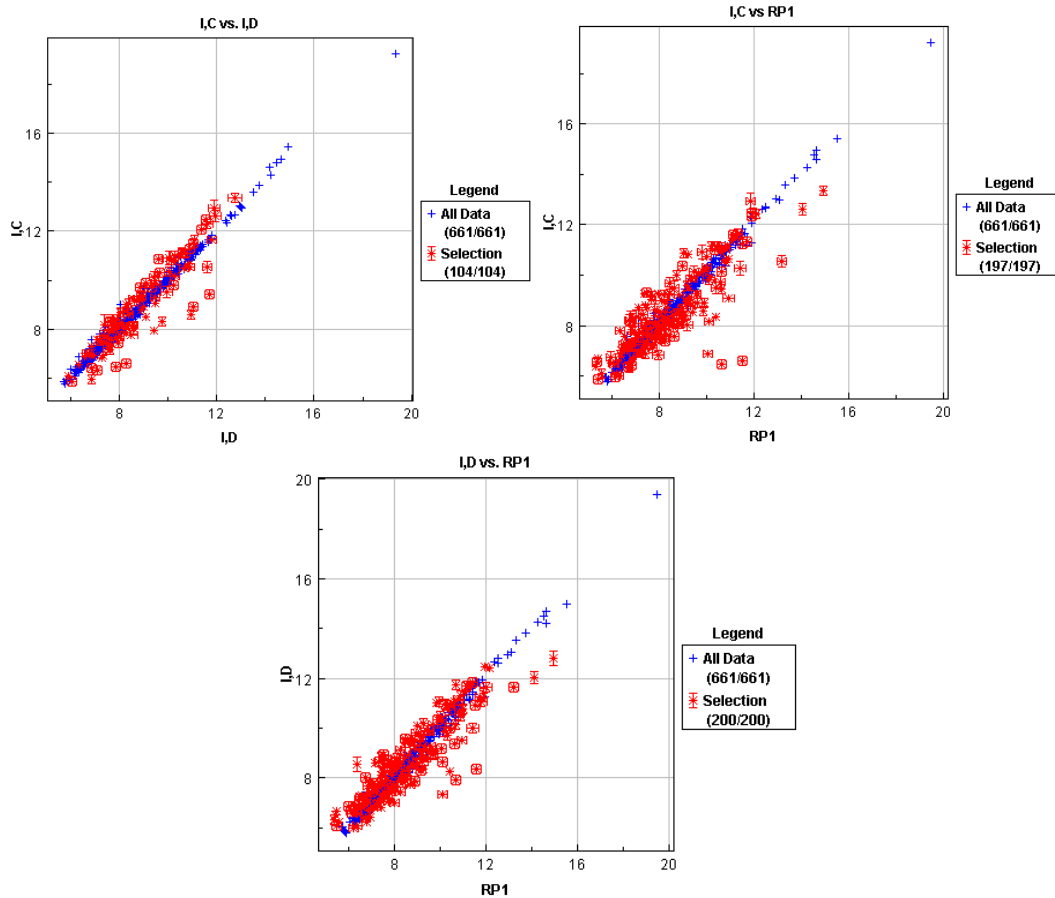


Figure 8. Scatter plots for pair-wise comparisons of selected miRNA hits following EW-ANOVA analysis for set “T”. Top left: pair-wise comparison for IC vs. ID samples; top right: pair-wise comparison for IC vs. NU samples; bottom center: pair-wise comparison for ID vs. NU.

In set ‘P’, there were only 16 miRNA probes that had significant differential expression in PC vs. PD comparison, 33 probes in PC vs. NU and 37 probes in PD vs. NU comparison.

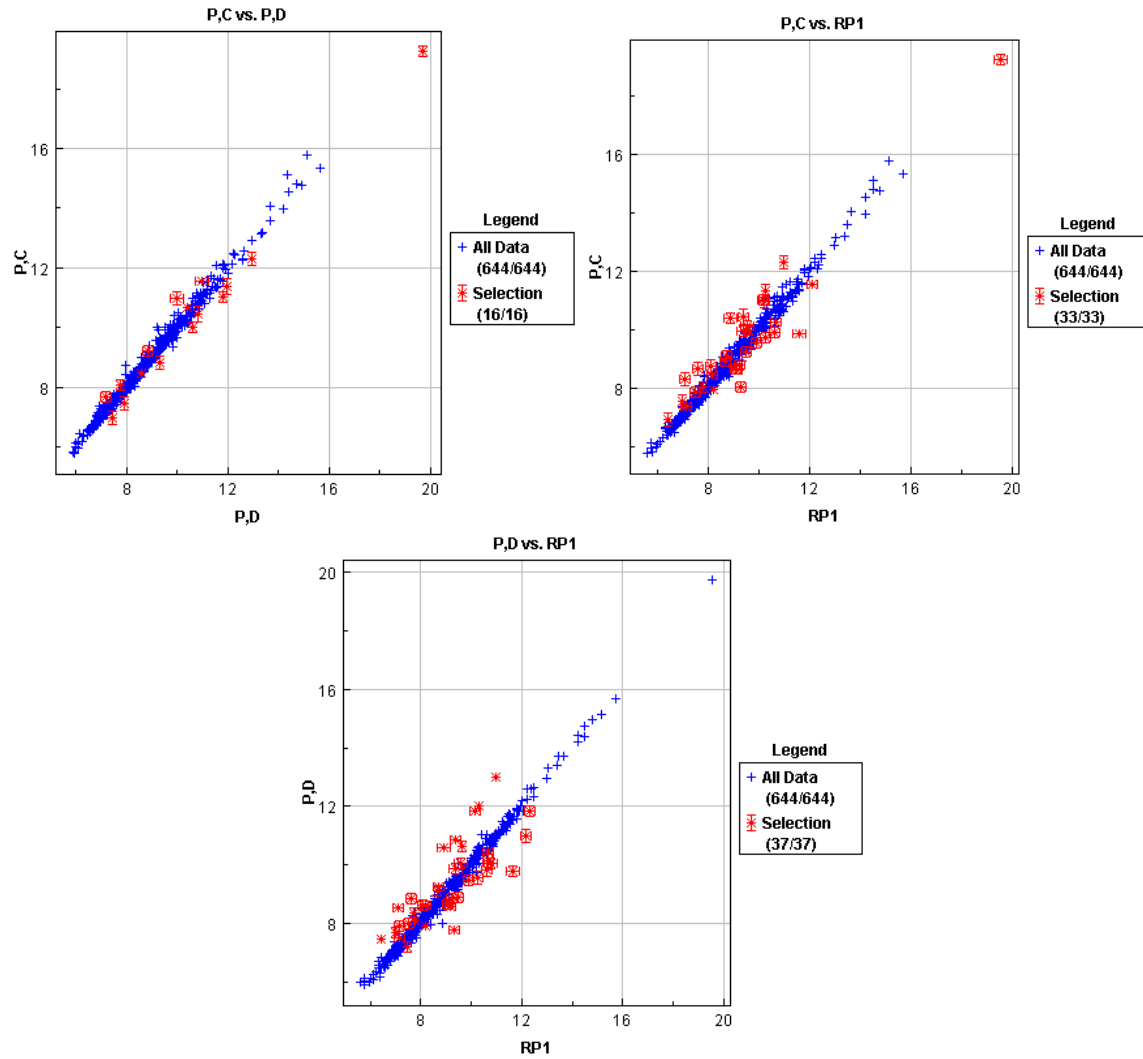


Figure 9. Scatter plots for pair-wise comparisons of selected miRNA hits following EW-ANOVA analysis for set “P”. Top left: pair-wise comparison for PC vs. PD samples; top right: pair-wise comparison for PC vs. NU samples; bottom center: pair-wise comparison for PD vs. NU samples.

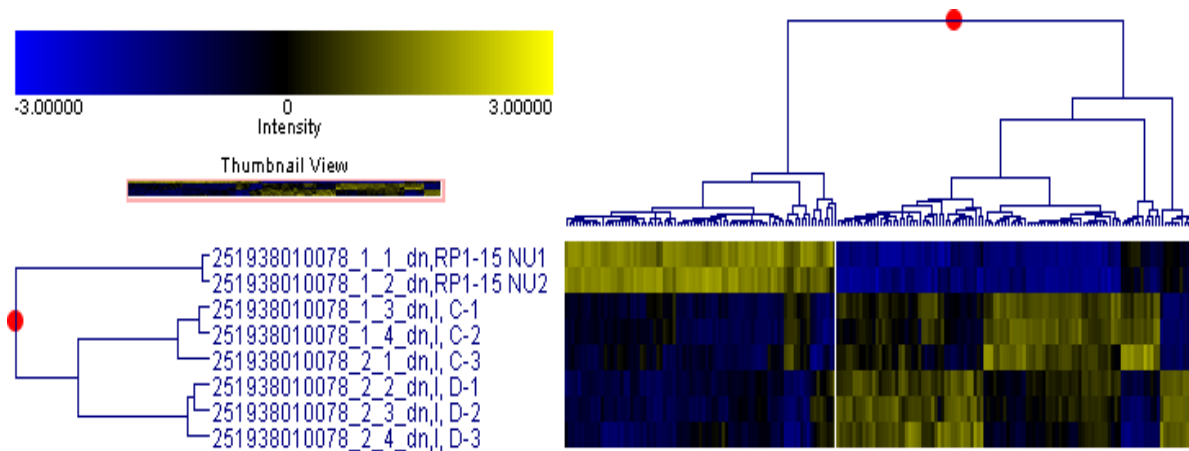


Figure 10. Hierarchical clustering with Z-transformed signals for set “I”.

A set of 222 miRNAs that had significant differential expression from set “I” was used for the cluster analysis (P^* value <0.01) as shown in [Figure 10](#).

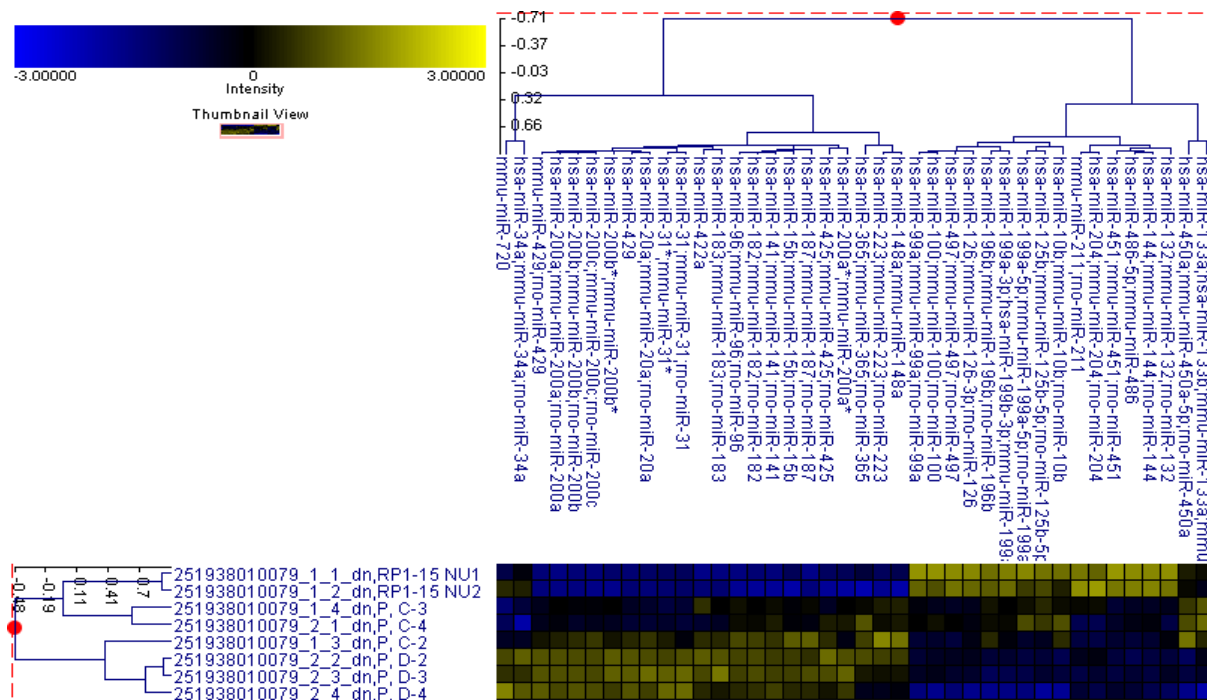


Figure 11. Hierarchical clustering with Z-transformed signals for set “P”.

A set of 40 miRNAs that had significant differential expression from set “P” was used for the cluster analysis (P^* value <0.01) as shown in [Figure 11](#). In the second case, only Control (C)

and DES (D) samples were used. Since each treatment factor has triplicate samples, a text book ANOVA could be performed and since the number of sample profiles is different, the number of miRNAs that pass statistical filtering is also expected to be different. The relative intensity data was subjected to statistical filtering resulting in 645 miRNA probes in the down stream analysis in set “I” and 635 miRNA probes in set “P”. This data was annotated, filtered, and log (2) scaled. The differential expression data was then used to perform text book ANOVA with FDR (false detection rate) multiple correction which reports a P*-value. The ANOVA results were then formatted into linear transformed values that show the fold-changes with a P*-value cut-off of 0.05. The fold-change data for the initiation stage and promotion stage can be found ins Tables 12 and 13.

TABLE 12

FOLD CHANGE DATA FOR INITIATION STAGE

Sequence Code	Factor	ID vs. IC	ID vs. IC	ID - IC	IC	ID	IC	ID
	Factor 1 P*-value	Fold Direction	Fold Change	Log Difference	Average	Average	Log(2) Average	Log(2) Average
hsa-miR-200b;mmu-miR-200b;rno-miR-200b	0.00154	Up	5.17	2.37104	366.4290315	1895.588371	8.51739	10.88843
hsa-miR-200a;mmu-miR-200a;rno-miR-200a	0.00367	Up	4.90	2.29259	643.9165855	3154.771939	9.33073	11.62332
mmu-miR-429;rno-miR-429	0.00367	Up	4.39	2.1339	450.4427672	1977.003898	8.8152	10.9491
hsa-miR-29a;mmu-miR-29a;rno-miR-29a	0.00367	Up	3.33	1.73533	91.25742241	303.8467394	6.51187	8.2472
hsa-miR-141;mmu-miR-141;rno-miR-141	0.00154	Up	2.94	1.55637	228.2862252	671.419208	7.8347	9.39107
hsa-miR-200c;mmu-miR-200c;rno-miR-200c	0.00367	Up	2.83	1.49929	292.5115943	826.9406616	8.19235	9.69164
hsa-miR-29b;mmu-miR-29b;rno-miR-29b	0.00367	Up	2.73	1.4505	82.66702137	225.9312464	6.36924	7.81974
hsa-miR-21;mmu-miR-21;rno-miR-21	0.02148	Up	2.04	1.02911	1429.336613	2916.940009	10.48113	11.51024
hsa-miR-429	0.00438	Up	1.93	0.95196	57.90275147	112.0128161	5.85556	6.80752
hsa-miR-155	0.00783	Up	1.75	0.80713	74.13022576	129.7076716	6.21199	7.01912
hsa-miR-31;mmu-miR-31;rno-miR-31	0.01615	Up	1.53	0.60969	342.41213	522.4973826	8.41959	9.02928
hsa-miR-30b;mmu-miR-30b;rno-miR-30b-5p	0.04793	Up	1.45	0.53439	162.4385225	235.2645273	7.34375	7.87814

TABLE 12 (CONT.)

hsa-miR-96;mmu-miR-96;rno-miR-96	0.04441	Up	1.43	0.518	132.9269666	190.347261	7.05449	7.57249
hsa-miR-22;mmu-miR-22;rno-miR-22	0.03507	Up	1.42	0.51087	505.3503086	720.0783095	8.98114	9.49201
hsa-miR-29c;mmu-miR-29c;rno-miR-29c	0.00438	Up	1.41	0.49686	106.9935487	150.9827585	6.74138	7.23824
hsa-miR-31*;mmu-miR-31*	0.03044	Up	1.41	0.49254	79.75317229	112.2063101	6.31747	6.81001
hsa-miR-200a*;mmu-miR-200a*	0.00154	Up	1.39	0.47987	114.1114698	159.141909	6.8343	7.31417
hsa-miR-200b*;mmu-miR-200b*	0.00783	Up	1.39	0.47801	217.0855669	302.3613656	7.76212	8.24013
hsa-miR-135a;mmu-miR-135a	0.03044	Up	1.37	0.45401	262.0975395	359.0323422	8.03396	8.48797
hsa-miR-182;mmu-miR-182;rno-miR-182	0.04441	Up	1.31	0.3897	196.0204008	256.8104324	7.61486	8.00456
hsa-miR-653;mmu-miR-653	0.03507	Up	1.22	0.29216	248.9409917	304.8213196	7.95966	8.25182
hsa-miR-208b;mmu-miR-208b	0.04967	Up	1.22	0.29163	140.2891865	171.7171115	7.13226	7.42389
hsa-miR-143*	0.04785	Up	1.19	0.25663	1427.168537	1705.016517	10.47894	10.73557
hsa-miR-542-5p;mmu-miR-542-5p;rno-miR-542-5p	0.04967	Up	1.18	0.24354	164.7232055	195.0148262	7.3639	7.60744
hsa-miR-135b*	0.01493	Up	1.17	0.2298	159.0900723	186.5605323	7.3137	7.5435
mmu-miR-290-5p;rno-miR-290	0.02148	Up	1.17	0.22146	499.5204736	582.3973577	8.9644	9.18586
mmu-miR-875-3p	0.04967	Up	1.16	0.20899	192.8065162	222.8609442	7.59101	7.8
hsa-miR-34c-5p;mmu-miR-34c;rno-miR-34c	0.0308	Up	1.16	0.20862	263.5531271	304.5573264	8.04195	8.25057
hsa-miR-585	0.02053	Up	1.15	0.19624	361.3517322	414.0037427	8.49726	8.6935
hsa-miR-519d	0.04363	Up	1.14	0.19385	89.9742334	102.9136117	6.49144	6.68529

TABLE 12 (CONT.)

hsa-miR-590-5p;mmu-miR-590-5p	0.02148	Up	1.13	0.17107	223.4425294	251.5724274	7.80376	7.97483
hsa-miR-769-5p	0.0127	Up	1.12	0.16211	92.58072787	103.5906513	6.53264	6.69475
mmu-miR-879;rno-miR-879	0.01706	Up	1.11	0.15012	3031.277048	3363.692246	11.56571	11.71583
hsa-miR-127-3p;mmu-miR-127;rno-miR-127	0.04182	Up	1.11	0.14749	176.2964972	195.2731794	7.46186	7.60935
hsa-miR-144*	0.04967	Up	1.09	0.12711	202.6097793	221.2709122	7.66256	7.78967
hsa-miR-376a;hsa-miR-376b	0.01565	Up	1.09	0.12589	151.0958264	164.8728459	7.23932	7.36521
hsa-miR-409-3p;mmu-miR-409-3p;rno-miR-409-3p	0.0245	Up	1.08	0.11271	155.3178681	167.9385935	7.27908	7.39179
hsa-miR-223*	0.04967	Up	1.08	0.10654	138.7044247	149.3351529	7.11587	7.22241
hsa-miR-124*;mmu-miR-124*;rno-miR-124*	0.02962	Up	1.08	0.10545	112.7989634	121.3524983	6.81761	6.92306
rno-miR-1*	0.04785	Up	1.07	0.10415	178.8107918	192.1967326	7.48229	7.58644
mmu-miR-434-5p	0.01706	Up	1.06	0.0865	128.4719863	136.4104161	7.00531	7.09181
hsa-miR-548a-3p	0.04263	Up	1.06	0.08421	144.1722806	152.8380557	7.17165	7.25586
hsa-miR-26a-1*	0.02499	Up	1.06	0.08125	139.1821125	147.2455271	7.12083	7.20208
hsa-miR-181a;mmu-miR-181a;rno-miR-181a	0.00783	Down	2.33	-1.21819	1748.400524	751.5003678	10.77182	9.55363
hsa-miR-125b;mmu-miR-125b-5p;rno-miR-125b-5p	0.03167	Down	1.90	-0.92758	5601.393242	2944.873607	12.45157	11.52399
hsa-miR-100;mmu-miR-100	0.01622	Down	1.75	-0.80836	775.9231715	443.0758856	9.59977	8.79141
hsa-miR-99a;mmu-miR-99a;rno-miR-99a	0.01799	Down	1.68	-0.74669	884.476499	527.120869	9.78868	9.04199
mmu-miR-669c	0.04441	Down	1.63	-0.7053	410.4463934	251.7329052	8.68105	7.97575
hsa-miR-221;mmu-miR-221;rno-miR-221	0.00367	Down	1.60	-0.68203	489.1489382	304.8804854	8.93413	8.2521
hsa-miR-10b;mmu-miR-10b;rno-miR-10b	0.02389	Down	1.57	-0.65248	1952.599024	1242.215707	10.93118	10.2787

TABLE 12 (CONT.)

hsa-miR-335;mmu-miR-335-5p;rno-miR-335	0.02126	Down	1.56	-0.64022	571.2268566	366.5077767	9.15792	8.517
hsa-miR-126;mmu-miR-126-3p;rno-miR-126	0.02283	Down	1.55	-0.63101	1217.891588	786.4220702	10.25017	9.61916
hsa-miR-181b;mmu-miR-181b;rno-miR-181b	0.01706	Down	1.53	-0.61528	497.0234118	324.458466	8.95717	8.34189
hsa-miR-130a;mmu-miR-130a;rno-miR-130a	0.01706	Down	1.50	-0.5846	1691.925114	1128.233528	10.72445	10.13985
hsa-miR-125a-5p;mmu-miR-125a-5p;rno-miR-125a-5p	0.01706	Down	1.44	-0.52592	2990.497922	2076.948891	11.54617	11.02025
hsa-let-7i;mmu-let-7i;rno-let-7i	0.035	Down	1.42	-0.50842	2134.244876	1500.35689	11.05951	10.55109
hsa-miR-181c;mmu-miR-181c;rno-miR-181c	0.01706	Down	1.42	-0.50707	386.4505475	271.9259454	8.59414	8.08707
hsa-miR-20a;mmu-miR-20a;rno-miR-20a	0.04785	Down	1.39	-0.47143	571.3575332	412.0912441	9.15825	8.68682
hsa-miR-25;mmu-miR-25;rno-miR-25	0.02263	Down	1.38	-0.46096	953.5204038	692.7351168	9.89712	9.43616
hsa-miR-93;mmu-miR-93;rno-miR-93	0.03093	Down	1.38	-0.45999	527.6801852	383.6189026	9.04352	8.58353
hsa-let-7e;mmu-let-7e;rno-let-7e	0.01706	Down	1.35	-0.43783	1968.785197	1453.44423	10.94309	10.50526
hsa-miR-181d;mmu-miR-181d;rno-miR-181d	0.04182	Down	1.35	-0.42883	412.6571993	306.5481738	8.6888	8.25997
hsa-miR-181a*;mmu-miR-181a-1*;rno-miR-181a*	0.01706	Down	1.33	-0.41138	175.6548986	132.0755859	7.4566	7.04522
hsa-miR-30e;mmu-miR-30e;rno-miR-30e	0.04441	Down	1.32	-0.40106	600.2875764	454.5987793	9.22951	8.82845
hsa-miR-224;mmu-miR-224;rno-miR-224	0.00438	Down	1.31	-0.38854	146.5165677	111.9243399	7.19492	6.80638

TABLE 12 (CONT.)

hsa-miR-10b*;mmu-miR-10b*	0.01398	Down	1.29	-0.36535	237.3660839	184.2626683	7.89097	7.52562
hsa-miR-199b-5p	0.03044	Down	1.25	-0.31647	880.9644547	707.4429501	9.78294	9.46647
hsa-miR-135b;mmu-miR-135b	0.02254	Down	1.19	-0.24553	109.3561085	92.24251861	6.77289	6.52736
mmu-miR-30b*;rno-miR-30b-3p	0.01706	Down	1.11	-0.15234	169.2462432	152.286052	7.40298	7.25064
hsa-miR-23b*	0.01706	Down	1.09	-0.12541	284.6726338	260.97178	8.15316	8.02775
hsa-miR-129-3p;hsa-miR-129*;mmu-miR-129-3p;rno-miR-129*	0.00783	Down	1.09	-0.1237	273.0459599	250.60997	8.093	7.9693
hsa-miR-296-3p;mmu-miR-296-3p;rno-miR-296	0.00367	Down	1.09	-0.11967	680.0891192	625.952772	9.40958	9.28991
mmu-miR-493	0.01706	Down	1.09	-0.11784	64.19415331	59.15917383	6.00437	5.88653
hsa-miR-320;mmu-miR-320;rno-miR-320	0.04441	Down	1.07	-0.10102	953.4741398	888.994079	9.89705	9.79603
hsa-miR-138-1*;mmu-miR-138*;rno-miR-138*	0.04441	Down	1.05	-0.07533	145.4803004	138.0789894	7.18468	7.10935

TABLE 13

FOLD CHANGE DATA FOR PROMOTION STAGE

Sequence Code	Factor	PD vs. PC	PD vs. PC	PD - PC	PC	PD	PC	PD
	Factor 1 P- value	Fold Directi on	Fold Change	Log Differen ce	Average	Average	Value	Value
mmu-miR-429;rno-miR-429	0.00514	Up	1.69	0.75854	2071.1696	3503.9586	11.01623	11.77477
hsa-miR-31;mmu-miR-31;rno-miR-31	0.00294	Up	1.60	0.67727	965.05008	1543.2221	9.91446	10.59173
hsa-miR-200b;mmu-miR-200b;rno-miR-200b	0.03111	Up	1.57	0.65241	2555.4648	4016.6582	11.31937	11.97178
hsa-miR-200a;mmu-miR-200a;rno-miR-200a	0.00536	Up	1.57	0.64905	4948.4809	7759.8874	12.27277	12.92182
hsa-miR-429	0.02846	Up	1.41	0.49902	121.78647	172.11512	6.92821	7.42723
mmu-miR-720	0.02052	Up	1.41	0.49669	626562.98	884063.21	19.2571	19.75379
hsa-miR-34a;mmu-miR-34a;rno-miR-34a	0.02588	Up	1.38	0.46342	453.65445	625.5017	8.82545	9.28887
hsa-miR-31*;mmu-miR-31*	0.02717	Up	1.35	0.42883	173.13217	233.06039	7.43573	7.86456
hsa-miR-615-5p;mmu-miR-615-5p	0.01597	Up	1.25	0.32694	1118.857	1403.4384	10.12781	10.45475
hsa-miR-431;mmu-miR-431;rno-miR-431	0.04568	Up	1.18	0.23321	315.29096	370.60795	8.30054	8.53375
hsa-miR-604	0.04106	Up	1.16	0.21776	2194.8247	2552.4199	11.09989	11.31765
mmu-miR-764-5p	0.04658	Up	1.14	0.19297	300.77691	343.82246	8.23255	8.42552
hsa-miR-200b*;mmu-miR-200b*	0.01199	Up	1.14	0.185	338.81408	385.16959	8.40435	8.58935
hsa-miR-649	0.03625	Up	1.14	0.18365	172.04355	195.3991	7.42663	7.61028
hsa-miR-626	0.04789	Up	1.11	0.14981	532.81098	591.11294	9.05748	9.20729

TABLE 13 (CONT.)

hsa-miR-539;mmu-miR-539;rno-miR-539	0.02834	Up	1.11	0.14933	202.1889	224.23847	7.65956	7.80889
hsa-miR-663	0.03603	Up	1.11	0.14811	2320.0015	2570.8327	11.17991	11.32802
hsa-miR-602	0.02403	Up	1.11	0.14586	549.84836	608.34672	9.10289	9.24875
mmu-miR-694	0.02431	Up	1.10	0.1402	141.55118	155.9976	7.14518	7.28538
hsa-miR-200a*;mmu-miR-200a*	0.00457	Up	1.09	0.1303	163.30442	178.74016	7.35142	7.48172
hsa-miR-33a;mmu-miR-33;rno-miR-33	0.04401	Up	1.08	0.11369	962.93193	1041.8848	9.91129	10.02498
hsa-miR-10a*;mmu-miR-10a*;rno-miR-10a-3p	0.03713	Up	1.08	0.1077	164.77459	177.54612	7.36435	7.47205
hsa-miR-135b*	0.03294	Up	1.07	0.10282	166.30296	178.58783	7.37767	7.48049
hsa-miR-627	0.01068	Up	1.07	0.09392	145.68818	155.48806	7.18674	7.28066
hsa-miR-223*	0.01504	Up	1.07	0.09313	144.15429	153.76678	7.17147	7.2646
mmu-miR-291a-5p;mmu-miR-291b-5p;rno-miR-291a-5p	0.03295	Up	1.06	0.09041	340.8398	362.88283	8.41295	8.50336
mmu-miR-302b*	0.04944	Up	1.06	0.0873	94.516873	100.41284	6.5625	6.6498
hsa-miR-218-2*;mmu-miR-218-2*;rno-miR-218*	0.03354	Up	1.05	0.07147	299.40199	314.60766	8.22594	8.29741
hsa-miR-329	0.01861	Up	1.04	0.06187	122.37966	127.74208	6.93522	6.99709
hsa-miR-133a	0.03711	Down	2.23	-1.1595	1773.8521	794.09621	10.79267	9.63317
hsa-miR-145*;mmu-miR-145*	0.03534	Down	1.85	-0.88383	988.6527	535.77743	9.94932	9.06549
hsa-miR-1;mmu-miR-1	0.03318	Down	1.74	-0.80086	427.46426	245.36744	8.73966	7.9388
hsa-miR-30c;mmu-miR-30c;rno-miR-30c	0.00935	Down	1.56	-0.64334	905.8887	579.97624	9.82319	9.17985
hsa-miR-29b;mmu-miR-29b;rno-miR-29b	0.02869	Down	1.45	-0.5389	2767.1018	1904.5837	11.43416	10.89526
hsa-miR-450a;mmu-miR-450a-5p;rno-miR-450a	0.00534	Down	1.44	-0.52676	201.61512	139.94344	7.65546	7.1287

TABLE 13 (CONT.)

hsa-miR-29a;mmu-miR-29a;rno-miR-29a	0.04405	Down	1.40	-0.4872	4011.7055	2861.9842	11.97	11.4828
hsa-miR-30b;mmu-miR-30b;rno-miR-30b-5p	0.02869	Down	1.39	-0.47002	640.36915	462.31745	9.32276	8.85274
hsa-miR-30a;mmu-miR-30a;rno-miR-29c	0.01968	Down	1.36	-	746.93557	550.16479	9.54484	9.10372
hsa-miR-29c;mmu-miR-29c;rno-miR-29c	0.03668	Down	1.35	-0.43714	1377.7706	1017.6177	10.42812	9.99098
hsa-miR-199a-3p;hsa-miR-199b-3p;mmu-miR-199a-3p;mmu-miR-199b;rno-miR-199a-3p	0.02761	Down	1.35	-0.43632	2912.7779	2152.5932	11.50818	11.07186
hsa-miR-517*	0.03122	Down	1.35	-0.43431	322.08775	238.36027	8.33131	7.897
hsa-miR-101;mmu-miR-101a;rno-miR-101a	0.03143	Down	1.34	-0.4205	1296.2246	968.49447	10.3401	9.9196
rno-miR-1	0.02955	Down	1.33	-0.41005	155.78689	117.24479	7.28343	6.87338
hsa-miR-30d;mmu-miR-30d;rno-miR-30d	0.02223	Down	1.30	-0.3806	983.85371	755.71581	9.9423	9.5617
hsa-miR-196b;mmu-miR-196b;rno-miR-196b	0.01351	Down	1.29	-0.36216	587.37172	456.97455	9.19813	8.83597
hsa-miR-24;mmu-miR-24;rno-miR-24	0.03101	Down	1.27	-0.34104	2768.7326	2185.8368	11.43501	11.09397
hsa-miR-424;mmu-miR-322;rno-miR-322	0.00673	Down	1.26	-0.33437	485.51094	385.07349	8.92336	8.58899
mmu-miR-199b*	0.03603	Down	1.26	-0.32978	1038.3809	826.19585	10.02012	9.69034
hsa-miR-125b;mmu-miR-125b-5p;rno-miR-125b-5p	0.04768	Down	1.25	-0.31838	4335.4018	3476.8618	12.08195	11.76357
hsa-miR-143*	0.0096	Down	1.18	-0.23872	2237.1093	1895.9432	11.12742	10.8887

TABLE 13 (CONT.),

hsa-miR-10b;mmu-miR-10b;rno-miR-10b	0.01872	Down	1.16	- 0.21844	1562.8786	1343.2853	10.60999	10.39155
hsa-miR-126*;mmu-miR-126-5p;rno-miR-126*	0.04839	Down	1.15	- 0.19783	476.97175	415.85305	8.89776	8.69993
mmu-miR-350;rno-miR-350	0.04556	Down	1.14	- 0.19018	324.96038	284.82659	8.34412	8.15394
hsa-miR-409-3p;mmu-miR-409-3p	0.01054	Down	1.13	-	165.40626	146.52774	7.36987	7.19503
hsa-let-7a*;mmu-let-7a*;mmu-let-	0.02533	Down	1.13	-	346.24994	307.74466	8.43567	8.26559
hsa-miR-491-3p	0.02524	Down	1.12	- 0.15853	154.53502	138.45372	7.27179	7.11326
hsa-miR-34b;mmu-miR-34b-3p	0.01227	Down	1.10	-0.1399	155.6552	141.26987	7.28221	7.14231
hsa-miR-130b;mmu-miR-130b;rno-miR-130b	0.0207	Down	1.10	- 0.13514	283.69364	258.32617	8.14819	8.01305
mmu-miR-34c*;rno-miR-34c*	0.0408	Down	1.10	- 0.13202	180.81242	165.00089	7.49835	7.36633
hsa-miR-708;mmu-miR-708;rno-miR-708	0.03017	Down	1.09	- 0.12594	167.33089	153.34316	7.38656	7.26062
hsa-miR-24-2*;mmu-miR-24-2*;rno-miR-24-2*	0.01809	Down	1.09	- 0.11894	220.02749	202.6154	7.78154	7.6626
hsa-miR-490-5p	0.01025	Down	1.05	- 0.06444	195.03646	186.51657	7.6076	7.54316

Out of 43 hits in the initiation-stage samples, only 8 miRNAs, miR-200b, miR-200a, miR-429, miR-29a, miR-141, miR-200c, miR-29b and miR-21 had two-fold or more up regulation and one miRNA, miR-181a had more than 2-fold down regulation. In the promotion-stage samples, only one miRNA, miR-133a, had more than 2-fold down regulation.

3.4 REAL-TIME PCR

TaqMan real-time PCR assays were used to independently assess the expression of miRNAs that had two-fold or more up-regulation or down-regulation in the initiation and promotion stages according to the microarray data. TaqMan miRNA assays specific for the targets discussed above were procured from Applied Biosystems. Plate design used the StepOne software, and RT-PCR was performed with a StepOne real time instrument and TaqMan Universal PCR master mix at 95°C for 10 min, at 95°C for 15 seconds, and 60°C for 1 minute for 40 cycles. The PCR cycling parameters are also illustrated in [Table 6](#). The real-time PCR was performed over the standard 2 hours for completing runs using the comparative C_T ($\Delta\Delta C_T$) method that gives differences in fold-change expression levels. For real-time PCR, cDNA obtained from the reverse transcription step was used as the template. The real-time PCR gives C_T values which are the cycle numbers at which the fluorescence within a reaction crosses the threshold. The C_T values are logarithmic and are used directly in the case of the $\Delta\Delta C_T$ method. The fluorescence threshold is set automatically by the instrument. Triplicate reactions were performed for each group of RNA samples from control and DES-exposed uteri. A no-melt curve was added because TaqMan reagents were used. Each assay generates a C_T value which was then used to calculate the ΔC_T value which normalizes the fluorescence of a miRNA of interest (MOI) to the endogenous control, Sno-RNA 202 (define what it is). The mean C_T value

for each replicate of the Sno-RNA 202 is subtracted from the mean C_T value of the unknown sample as shown in the illustration below,

$$\Delta C_T = C_T (\text{MOI}) - C_T (\text{Sno-RNA 202})$$

In the next step, $\Delta\Delta C_T$ value was calculated as in the following equation,

$$\Delta\Delta C_T = \Delta C_T \text{ DES} - \Delta C_T \text{ CONTROL}$$

The miRNA expression given by ΔC_T values represented by $\Delta C_T \pm \text{SEM}$ is summarized in Table 14 and illustrated in the graph shown in Figure 12 and the statistical significance was measured using student's t-test with a cut-off limit of $p < 0.05$.

TABLE 14

ΔC_T VALUES \pm SEM (>2-FOLD DIFFERENCE)

miRNA	$\Delta C_T(\text{CON})$	SEM(CON)	$\Delta C_T(\text{DES})$	SEM(DES)
miR-21	3.32	0.18	1.85	0.24
miR-200a	2.28	0.31	-0.19	0.17
miR-200b	3.50	0.17	0.95	0.32
miR-200c	4.46	0.32	2.72	0.19
miR-29a	4.61	0.17	2.18	0.58
miR-29b	9.98	0.30	6.19	0.33
miR-429	5.25	0.38	2.87	0.55
miR-141	5.13	0.06	3.72	0.34
miR-181a	1.12	0.17	2.89	0.19

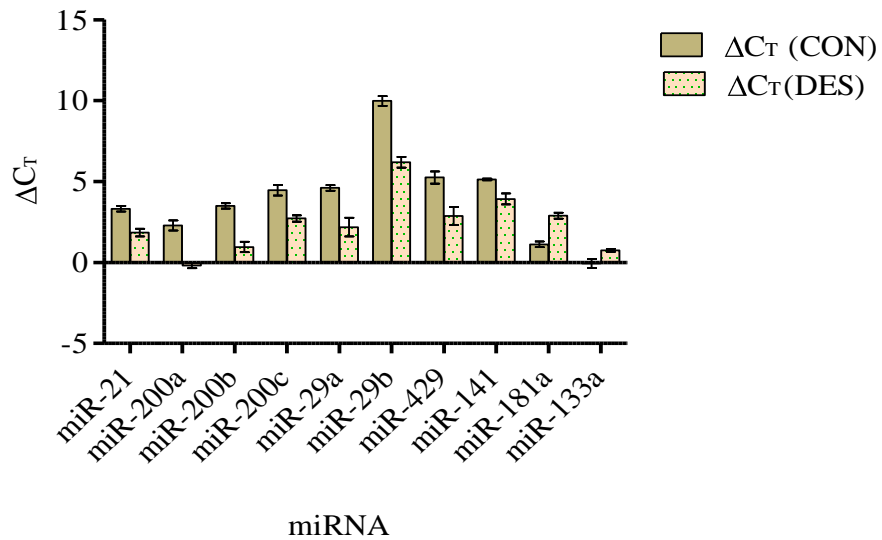


Figure 12. MiRNA expression in total RNA samples from control and DES-exposed uteri shown as ΔC_T values. With this representation method, the smaller the ΔC_T value, the higher the target expression level. According to student's t-test, mean differences in ΔC_T between the control and DES groups were significant for all targets except miR-133a.

To further confirm the microarray results, two microRNAs (miR-10b and miR-133b), were assessed by RT-PCR that had less than 2-fold change in expression levels according to microarray in both the initiation and promotion stage samples. [Figure 13](#) illustrates the miRNA expression as ΔC_T values. The ΔC_T values \pm SEM for these two miRNAs are also shown in [Table 15](#). The statistical significance was tested using student's t-test with a p-value cut off of 0.05. Consistent with the microarray analysis, RT-PCR also indicated that expression of those miRNAs was not significantly different in the RNA samples of CON vs. DES-exposed uterine tissues at either the initiation or promotion stages of the neoplastic phenomenon.

TABLE 15

ΔC_T VALUES +/- SEM (<2-FOLD DIFFERENCE)

miRNA	ΔC_T (CON)	SEM(CON)	ΔC_T (DES)	SEM(DES)
miR-10b (I)	2.02	0.21	2.23	0.01
miR-10b (P)	4.30	0.30	3.93	0.21
miR-130b (I)	4.41	0.19	5.08	0.08
miR-130b (P)	7.58	0.19	7.82	0.27

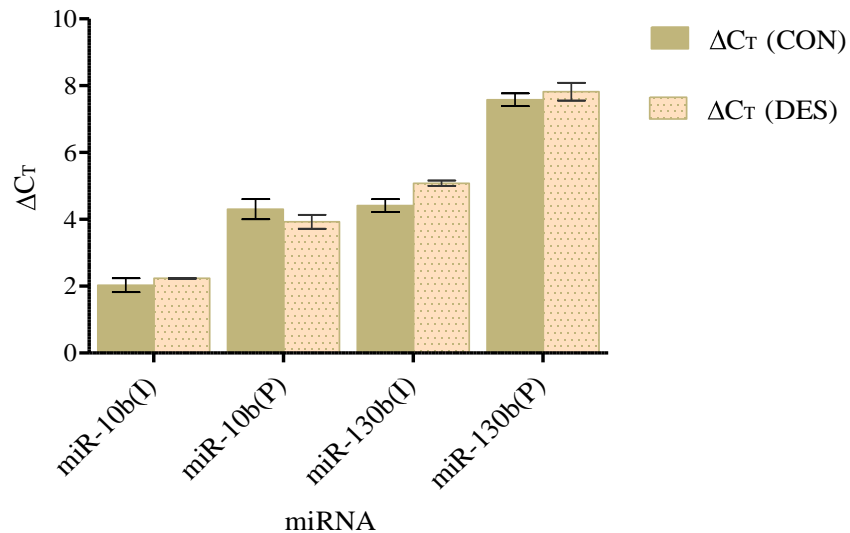


Figure 13. MiR-10b and miR-130b expression in total RNA samples of control and DES-exposed uteri shown as ΔC_T values.

The fold change in expression levels was calculated relative to the control according to the following equation,

$$\text{Fold-change} = 2^{-\Delta C_T}$$

If the fold-change value is greater than 1, then the value is expressed as fold-up regulation and if the value is less than 1, the fold-change is expressed as the negative inverse of the value. The

fold-change comparison between miRNA microarray and TaqMan miRNA RT-PCR assay is illustrated in the graph shown in [Figure 14](#). Most of the microarray and RT-PCR results were comparable, the most obvious exception being miR-29b. The overall pattern of DES-treatment differential expression was primarily (8 out of 10) up-regulated in nature. Only one of them (miR-133a) exceeded or approached the two-fold differential expression level in the promotion stage samples according to both assay methods. MiR-181a, the down-regulated miRNA at the initiation stage also showed down-regulation in the RT-PCR assay. Though miR-133a showed down-regulation in the RT-PCR assay, the fold-change was less than 2 and was not statistically significant.

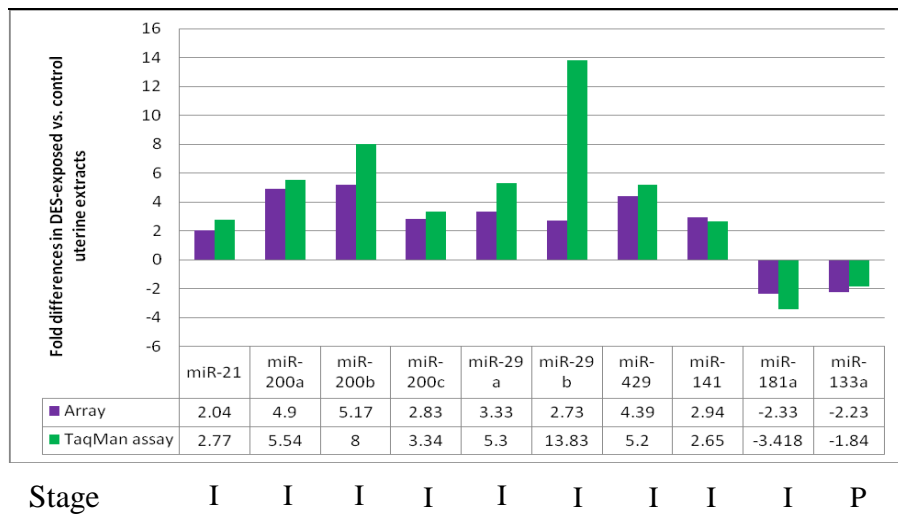


Figure 14. Comparison of neonatal DES treatment-dependent differences in miRNA expression (≥ 2 -fold) according to microarray vs. RT-PCR assays. I: Initiation; P: Promotion.

CHAPTER 4

CONCLUSION AND FUTURE DIRECTIONS

Using specific and sensitive microarray and RT-PCR assays, the current study compliments other assessments at the mRNA and protein levels (Altered gene expression patterns during the initiation and promotion stages of neonatal diethylstilbestrol-induced dysplasia/ neoplasia in the hamster uterus, W. J. Hendry et al. In preparation) that neonatal exposure to the synthetic estrogen, diethylstilbestrol, involves a series of gene expression alterations at multiple levels. The number of miRNAs that showed differential expression at both stages was different. Furthermore, miRNA RT-PCR assays using the comparative (ΔC_T) method validated the microarray results. RT-PCR assays can be considered more sensitive and specific than microarray analyses because microarrays tend to produce greater background fluorescence intensity levels. Of the 43 up-regulated miRNAs at the initiation stage, 8 miRNAs [miR-21, miR-200 family (miR-141, miR-200a, miR-200b, miR-200c and miR-429), miR-29a, and miR-29b] had more than 2-fold up-regulation. Of the 32 miRNAs down-regulated at the initiation stage, only miR-181a had more than 2-fold down-regulation. Though there were 29 miRNAs that were up-regulated at the promotion stage, none were 2-fold up-regulated and only miR-133a was 2-fold down-regulated. This difference in degree of differential miRNA expression detected in the initiation vs. promotion-stage samples could be due to the facts that they represented whole-organ extracts and that there are dramatic differences in terms of overall histological complexities plus pronounced epithelial-stromal interactions, and other vascular and hormonal changes in a 2-month-old uterus compared to a 5-day-old uterus. For instance, by day 5 after neonatal DES-exposure, the uterine epithelium shows some hypertrophy and degree of pseudostratified organization [75, 81, 82]. However, the 2-month old uteri show advanced

hypertrophy together with dysplastic histomorphology. Additionally, cavities harboring apoptotic bodies increase the distortions. In advanced stages, the DES-exposed uterine epithelium also shows poor demarcation from the underlying stromal layer [75].

MiR-200b and miR-29b were 8- and 13.83-fold up-regulated in the RT-PCR assays as opposed to 5.17- and 2.73-fold up-regulated in the microarray analyses, while the other values were much closer according to both assessment methods. It is worthwhile to note (from the validation assays of less than 2- fold differentially expressed miRNAs) that: 1) miR-10b had 1.10-fold down-regulation in RT-PCR assay and 1.57-fold down-regulation in microarray analysis at the initiation stage. 2) miR-10b had 1.29- fold up-regulation at the promotion stage in RT-PCR assays and 1.16 fold- down-regulation in microarray analysis. 3) MiR-130b (which was not listed at the initiation stage in microarray analysis), was down-regulated 1.59 times in RT-PCR assay and 4) miR-130b which had 1.10- fold down-regulation in microarray analysis and 1.18-fold down-regulation in the RT-PCR assays at the promotion stage. In other words, the microarray vs. PCR assay results for all those miRNA targets in both the initiation and promotion sets of samples were very similar.

Of the 8 up-regulated miRNAs at the initiation stage, the miR-200 family members are evolutionarily conserved miRNAs that are localized in epithelial tissues. [83]. The latter point is significant in view of the fact that cancer mainly arises from epithelial tissues. Therefore, these miRNAs might be involved in the molecular mechanisms including changes in gene expression in neoplastic alterations detected in the hamster uterus following neonatal DES exposure. Epithelial-mesenchymal transition (EMT) occurs as part of various processes in embryonic development [84] and during tumor invasion and metastasis [85]. The miR-200 family directly targets the E-cadherin repressors ZEB1 and ZEB2 [83]. The metastatic process involves

epithelial-mesenchymal transitions that enhance the mobility of cancer cells [86]. Over expression of the miR-200 cluster or individual members inhibited EMT by enhancing the synthesis of E-cadherin through negative regulation of ZEB1 and ZEB2 [87]. However, this contrasts with the current study where miR-200 family miRNAs were up-regulated at the initiation stage and up-regulation leads to the reverse process of EMT, mesenchymal-epithelial transition (MET), that is correlated with decreased cell motility and reduced metastasis. In DES-induced carcinogenic phenomenon, the mRNA targets involved could be different. Increased understanding and identification of mRNAs targeted by the miR-200 family will further clarify their roles in the carcinogenesis process. MiR-21 is a multifaceted miRNA that acts as an oncogene by inhibiting various mRNAs coding for tumor suppressor proteins as described earlier. The important targets of miR-21 include programmed cell death protein 4 (PDCD4), reversion-inducing cysteine-rich protein (RECK), and tropomyosin 1 (TPM1). Regulation of PDCD4 by miR-21 is reported in breast cancer [88], colorectal cancer [89], lung cancer [90], and colon cancer [91]. Up-regulation of miR-21 by more than 2-fold at the initiation stage strongly supports its role in the DES-induced carcinogenic process. The miR-29 family includes miR-29a, miR-29b and miR-29c. MiR-29a negatively regulates tristetraprolin (TTP), a protein that degrades mRNAs with AU-rich 3'-UTR's [92]. Over expression of miR-29a led to increased EMT and metastasis in breast cancer samples. This observation is encouraging and can be extended to DES-induced carcinogenesis. MiR-29b has perfect complementarity to 3' UTR of the anti-apoptotic Mcl-1 mRNA, a Bcl-2 family protein [93]. High expression of miR-29b was found in immortalized but non-malignant H69 cholangiocytes indicating the role of Mcl-2 protein regulation by miR-29b. But miR-29b was down-regulated in cholangiocarcinoma cell lines consistent with Mcl-1 protein up-regulation. MiR-181a functions as a tumor suppressor in

human glioma cells [94] as down-regulation of miR-181a contributed to malignancy in human glioma. miR-181a also functions in regulating the cell cycle regulator and tumor suppressor protein p27 [95]. MiR-181a expression is down-regulated during terminal differentiation of HL60 (human promyelocytic leukemia) cells into monocyte-like cells. This relieves the suppression of p27 and leads to cell differentiation. As already discussed, miR-181a is also regulated by estrogen and progesterone levels in the endometrial epithelium and targets many genes including estrogen and progesterone receptors and aromatase [39]. The down-regulation of miR-181a at the initiation stage suggests that loss of tumor suppressor function by this miRNA leads to progression of cancer. Further studies may reveal more important roles of miR-181a in DES-induced endometrial cancer. Detailed understanding of the putative targets of these miRNAs may also reveal their roles in other hormone-dependent cancers.

Recent studies conducted by Mitchell et al [96] reported the presence of tumor-derived circulating miRNAs in blood that can be used as a blood-based diagnostic technique to detect human cancers. Using PAGE and phosphorimaging of radiolabeled plasma RNA, they demonstrated the presence of miRNAs corresponding to the size of precursors as well as mature sequences. To check if cancer-derived miRNAs enter the circulation, they used a mouse model xenografted with the prostate cancer cell line 22Rv1. Before conducting profiling of the xenografted mouse, they sought to find candidate tumor-derived miRNAs by conducting profiling for 365 known targets in the cancer cell line. Two miRNAs, miR-629 and miR-660, were found over expressed and they were readily detectable in the plasma of all xenografted mice. This suggests that a reasonable next step for us might be to investigate if any of the miRNAs differentially expressed in the current profiling study could be detected in blood

REFERENCES

LIST OF REFERENCES

1. Fire A, Xu S, Montgomery MK, Kostas SA, Driver SE, Mello CC. Potent and specific genetic interference by double-stranded RNA in *Caenorhabditis elegans*. *Nature* 1998; 391: 806-811.
2. Napoli C, Lemieux C, Jorgensen R. Introduction of a Chimeric Chalcone Synthase Gene into *Petunia* Results in Reversible Co-Suppression of Homologous Genes in trans. *Plant Cell* 1990; 2: 279-289.
3. Cogoni C, Irelan JT, Schumacher M, Schmidhauser TJ, Selker EU, Macino G. Transgene silencing of the *al-1* gene in vegetative cells of *Neurospora* is mediated by a cytoplasmic effector and does not depend on DNA-DNA interactions or DNA methylation. *EMBO J* 1996; 15: 3153-3163.
4. Lindbo JA, Dougherty WG. Untranslatable transcripts of the tobacco etch virus coat protein gene sequence can interfere with tobacco etch virus replication in transgenic plants and protoplasts. *Virology* 1992; 189: 725-733.
5. Bartel DP. MicroRNAs: genomics, biogenesis, mechanism, and function. *Cell* 2004; 116: 281-297.
6. Esquela-Kerscher A, Slack FJ. Oncomirs - microRNAs with a role in cancer. *Nat Rev Cancer* 2006; 6: 259-269.
7. Griffiths-Jones S. The microRNA Registry. *Nucleic Acids Res* 2004; 32: D109-111.
8. Jovanovic M, Hengartner MO. miRNAs and apoptosis: RNAs to die for. *Oncogene* 2006; 25: 6176-6187.
9. Lee RC, Feinbaum RL, Ambros V. The *C. elegans* heterochronic gene *lin-4* encodes small RNAs with antisense complementarity to *lin-14*. *Cell* 1993; 75: 843-854.
10. Wightman B, Ha I, Ruvkun G. Posttranscriptional regulation of the heterochronic gene *lin-14* by *lin-4* mediates temporal pattern formation in *C. elegans*. *Cell* 1993; 75: 855-862.
11. Reinhart BJ, Slack FJ, Basson M, Pasquinelli AE, Bettinger JC, Rougvié AE, Horvitz HR, Ruvkun G. The 21-nucleotide *let-7* RNA regulates developmental timing in *Caenorhabditis elegans*. *Nature* 2000; 403: 901-906.
12. Brennecke J, Hipfner DR, Stark A, Russell RB, Cohen SM. *bantam* encodes a developmentally regulated microRNA that controls cell proliferation and regulates the proapoptotic gene *hid* in *Drosophila*. *Cell* 2003; 113: 25-36.

13. Poy MN, Eliasson L, Krutzfeldt J, Kuwajima S, Ma X, Macdonald PE, Pfeffer S, Tuschl T, Rajewsky N, Rorsman P, Stoffel M. A pancreatic islet-specific microRNA regulates insulin secretion. *Nature* 2004; 432: 226-230.
14. Xu P, Vernooij SY, Guo M, Hay BA. The *Drosophila* microRNA Mir-14 suppresses cell death and is required for normal fat metabolism. *Curr Biol* 2003; 13: 790-795.
15. Johnston RJ, Hobert O. A microRNA controlling left/right neuronal asymmetry in *Caenorhabditis elegans*. *Nature* 2003; 426: 845-849.
16. He L, Hannon GJ. MicroRNAs: small RNAs with a big role in gene regulation. *Nat Rev Genet* 2004; 5: 522-531.
17. Cullen BR. Transcription and processing of human microRNA precursors. *Mol Cell* 2004; 16: 861-865.
18. Yi R, Qin Y, Macara IG, Cullen BR. Exportin-5 mediates the nuclear export of pre-microRNAs and short hairpin RNAs. *Genes Dev* 2003; 17: 3011-3016.
19. Kim VN. MicroRNA biogenesis: coordinated cropping and dicing. *Nat Rev Mol Cell Biol* 2005; 6: 376-385.
20. Roy AK, Oh T, Rivera O, Mubiru J, Song CS, Chatterjee B. Impacts of transcriptional regulation on aging and senescence. *Ageing Res Rev* 2002; 1: 367-380.
21. Yang WJ, Yang DD, Na S, Sandusky GE, Zhang Q, Zhao G. Dicer is required for embryonic angiogenesis during mouse development. *J Biol Chem* 2005; 280: 9330-9335.
22. Williams AE, Moschos SA, Perry MM, Barnes PJ, Lindsay MA. Maternally imprinted microRNAs are differentially expressed during mouse and human lung development. *Dev Dyn* 2007; 236: 572-580.
23. Williams AE, Perry MM, Moschos SA, Lindsay MA. microRNA expression in the aging mouse lung. *BMC Genomics* 2007; 8: 172.
24. Boehm M, Slack F. A developmental timing microRNA and its target regulate life span in *C. elegans*. *Science* 2005; 310: 1954-1957.
25. Chen JF, Murchison EP, Tang R, Callis TE, Tatsuguchi M, Deng Z, Rojas M, Hammond SM, Schneider MD, Selzman CH, Meissner G, Patterson C, Hannon GJ, Wang DZ. Targeted deletion of Dicer in the heart leads to dilated cardiomyopathy and heart failure. *Proc Natl Acad Sci U S A* 2008; 105: 2111-2116.

26. van Rooij E, Sutherland LB, Liu N, Williams AH, McAnally J, Gerard RD, Richardson JA, Olson EN. A signature pattern of stress-responsive microRNAs that can evoke cardiac hypertrophy and heart failure. *Proc Natl Acad Sci U S A* 2006; 103: 18255-18260.
27. Kosik KS, Krichevsky AM. The Elegance of the MicroRNAs: A Neuronal Perspective. *Neuron* 2005; 47: 779-782.
28. Visvanathan J, Lee S, Lee B, Lee JW, Lee SK. The microRNA miR-124 antagonizes the anti-neural REST/SCP1 pathway during embryonic CNS development. *Genes Dev* 2007; 21: 744-749.
29. Hebert SS, Horre K, Nicolai L, Papadopoulou AS, Mandemakers W, Silaharoglu AN, Kauppinen S, Delacourte A, De Strooper B. Loss of microRNA cluster miR-29a/b-1 in sporadic Alzheimer's disease correlates with increased BACE1/beta-secretase expression. *Proc Natl Acad Sci U S A* 2008; 105: 6415-6420.
30. Kim J, Inoue K, Ishii J, Vanti WB, Voronov SV, Murchison E, Hannon G, Abeliovich A. A MicroRNA feedback circuit in midbrain dopamine neurons. *Science* 2007; 317: 1220-1224.
31. Lindsay MA. microRNAs and the immune response. *Trends Immunol* 2008; 29: 343-351.
32. Gantier MP, Sadler AJ, Williams BR. Fine-tuning of the innate immune response by microRNAs. *Immunol Cell Biol* 2007; 85: 458-462.
33. Sonkoly E, Wei T, Janson PC, Saaf A, Lundeberg L, Tengvall-Linder M, Norstedt G, Alenius H, Homey B, Scheynius A, Stahle M, Pivarcsi A. MicroRNAs: novel regulators involved in the pathogenesis of Psoriasis? *PLoS ONE* 2007; 2: e610.
34. Tan Z, Randall G, Fan J, Camoretti-Mercado B, Brockman-Schneider R, Pan L, Solway J, Gern JE, Lemanske RF, Nicolae D, Ober C. Allele-specific targeting of microRNAs to HLA-G and risk of asthma. *Am J Hum Genet* 2007; 81: 829-834.
35. Nakasa T, Miyaki S, Okubo A, Hashimoto M, Nishida K, Ochi M, Asahara H. Expression of microRNA-146 in rheumatoid arthritis synovial tissue. *Arthritis Rheum* 2008; 58: 1284-1292.
36. Harris TA, Yamakuchi M, Ferlito M, Mendell JT, Lowenstein CJ. MicroRNA-126 regulates endothelial expression of vascular cell adhesion molecule 1. *Proc Natl Acad Sci U S A* 2008; 105: 1516-1521.
37. Thai TH, Calado DP, Casola S, Ansel KM, Xiao C, Xue Y, Murphy A, Frendewey D, Valenzuela D, Kutok JL, Schmidt-Supprian M, Rajewsky N, Yancopoulos G, Rao A, Rajewsky K. Regulation of the germinal center response by microRNA-155. *Science* 2007; 316: 604-608.

38. Toloubeydokhti T, Pan Q, Luo X, Bukulmez O, Chegini N. The expression and ovarian steroid regulation of endometrial micro-RNAs. *Reprod Sci* 2008; 15: 993-1001.
39. Pan Q, Chegini N. MicroRNA signature and regulatory functions in the endometrium during normal and disease states. *Semin Reprod Med* 2008; 26: 479-493.
40. Hong XM, Luense LJ, McGinnis LK, Nothnick WB, Christenson LK. Dicer1 Is Essential for Female Fertility and Normal Development of the Female Reproductive System. *Endocrinology* 2008; 149: 6207-6212.
41. Yu SL, Chen HY, Yang PC, Chen JJ. Unique MicroRNA signature and clinical outcome of cancers. *DNA Cell Biol* 2007; 26: 283-292.
42. Calin GA, Sevignani C, Dumitru CD, Hyslop T, Noch E, Yendamuri S, Shimizu M, Rattan S, Bullrich F, Negrini M, Croce CM. Human microRNA genes are frequently located at fragile sites and genomic regions involved in cancers. *Proc Natl Acad Sci U S A* 2004; 101: 2999-3004.
43. Zhang W, Dahlberg JE, Tam W. MicroRNAs in tumorigenesis: a primer. *Am J Pathol* 2007; 171: 728-738.
44. Calin GA, Dumitru CD, Shimizu M, Bichi R, Zupo S, Noch E, Aldler H, Rattan S, Keating M, Rai K, Rassenti L, Kipps T, Negrini M, Bullrich F, Croce CM. Frequent deletions and down-regulation of micro- RNA genes miR15 and miR16 at 13q14 in chronic lymphocytic leukemia. *Proc Natl Acad Sci U S A* 2002; 99: 15524-15529.
45. Cimmino A, Calin GA, Fabbri M, Iorio MV, Ferracin M, Shimizu M, Wojcik SE, Aqeilan RI, Zupo S, Dono M, Rassenti L, Alder H, Volinia S, Liu CG, Kipps TJ, Negrini M, Croce CM. miR-15 and miR-16 induce apoptosis by targeting BCL2. *Proc Natl Acad Sci U S A* 2005; 102: 13944-13949.
46. Iorio MV, Ferracin M, Liu CG, Veronese A, Spizzo R, Sabbioni S, Magri E, Pedriali M, Fabbri M, Campiglio M, Menard S, Palazzo JP, Rosenberg A, Musiani P, Volinia S, Nenci I, Calin GA, Querzoli P, Negrini M, Croce CM. MicroRNA gene expression deregulation in human breast cancer. *Cancer Res* 2005; 65: 7065-7070.
47. Tam W, Ben-Yehuda D, Hayward WS. bic, a novel gene activated by proviral insertions in avian leukosis virus-induced lymphomas, is likely to function through its noncoding RNA. *Mol Cell Biol* 1997; 17: 1490-1502.
48. Eis PS, Tam W, Sun L, Chadburn A, Li Z, Gomez MF, Lund E, Dahlberg JE. Accumulation of miR-155 and BIC RNA in human B cell lymphomas. *Proc Natl Acad Sci U S A* 2005; 102: 3627-3632.

49. Lee EJ, Gusev Y, Jiang J, Nuovo GJ, Lerner MR, Frankel WL, Morgan DL, Postier RG, Brackett DJ, Schmittgen TD. Expression profiling identifies microRNA signature in pancreatic cancer. *Int J Cancer* 2007; 120: 1046-1054.
50. Welch C, Chen Y, Stallings RL. MicroRNA-34a functions as a potential tumor suppressor by inducing apoptosis in neuroblastoma cells. *Oncogene* 2007; 26: 5017-5022.
51. Thomson JM, Newman M, Parker JS, Morin-Kensicki EM, Wright T, Hammond SM. Extensive post-transcriptional regulation of microRNAs and its implications for cancer. *Genes Dev* 2006; 20: 2202-2207.
52. Karube Y, Tanaka H, Osada H, Tomida S, Tatematsu Y, Yanagisawa K, Yatabe Y, Takamizawa J, Miyoshi S, Mitsudomi T, Takahashi T. Reduced expression of Dicer associated with poor prognosis in lung cancer patients. *Cancer Sci* 2005; 96: 111-115.
53. Calin GA, Croce CM. MicroRNA signatures in human cancers. *Nat Rev Cancer* 2006; 6: 857-866.
54. Liu CG, Calin GA, Meloon B, Gamliel N, Sevignani C, Ferracin M, Dumitru CD, Shimizu M, Zupo S, Dono M, Alder H, Bullrich F, Negrini M, Croce CM. An oligonucleotide microchip for genome-wide microRNA profiling in human and mouse tissues. *Proc Natl Acad Sci U S A* 2004; 101: 9740-9744.
55. Valoczi A, Hornyik C, Varga N, Burgyan J, Kauppinen S, Havelda Z. Sensitive and specific detection of microRNAs by northern blot analysis using LNA-modified oligonucleotide probes. *Nucleic Acids Res* 2004; 32: e175.
56. Cummins JM, He Y, Leary RJ, Pagliarini R, Diaz LA, Jr., Sjoblom T, Barad O, Bentwich Z, Szafranska AE, Labourier E, Raymond CK, Roberts BS, Juhl H, Kinzler KW, Vogelstein B, Velculescu VE. The colorectal microRNAome. *Proc Natl Acad Sci U S A* 2006; 103: 3687-3692.
57. Volinia S, Calin GA, Liu CG, Ambs S, Cimmino A, Petrocca F, Visone R, Iorio M, Roldo C, Ferracin M, Prueitt RL, Yanaihara N, Lanza G, Scarpa A, Vecchione A, Negrini M, Harris CC, Croce CM. A microRNA expression signature of human solid tumors defines cancer gene targets. *Proc Natl Acad Sci U S A* 2006; 103: 2257-2261.
58. Ciafre SA, Galardi S, Mangiola A, Ferracin M, Liu CG, Sabatino G, Negrini M, Maira G, Croce CM, Farace MG. Extensive modulation of a set of microRNAs in primary glioblastoma. *Biochem Biophys Res Commun* 2005; 334: 1351-1358.
59. Murakami Y, Yasuda T, Saigo K, Urashima T, Toyoda H, Okanoue T, Shimotohno K. Comprehensive analysis of microRNA expression patterns in hepatocellular carcinoma and non-tumorous tissues. *Oncogene* 2006; 25: 2537-2545.

60. Meng F, Henson R, Lang M, Wehbe H, Maheshwari S, Mendell JT, Jiang J, Schmittgen TD, Patel T. Involvement of human micro-RNA in growth and response to chemotherapy in human cholangiocarcinoma cell lines. *Gastroenterology* 2006; 130: 2113-2129.
61. He H, Jazdzewski K, Li W, Liyanarachchi S, Nagy R, Volinia S, Calin GA, Liu CG, Franssila K, Suster S, Kloos RT, Croce CM, de la Chapelle A. The role of microRNA genes in papillary thyroid carcinoma. *Proc Natl Acad Sci U S A* 2005; 102: 19075-19080.
62. Wang T, Zhang X, Obijuru L, Laser J, Aris V, Lee P, Mittal K, Soteropoulos P, Wei JJ. A micro-RNA signature associated with race, tumor size, and target gene activity in human uterine leiomyomas. *Genes Chromosomes Cancer* 2007; 46: 336-347.
63. Zhang Z, Li Z, Gao C, Chen P, Chen J, Liu W, Xiao S, Lu H. miR-21 plays a pivotal role in gastric cancer pathogenesis and progression. *Lab Invest* 2008; 88: 1358-1366.
64. Meng F, Henson R, Wehbe-Janek H, Ghoshal K, Jacob ST, Patel T. MicroRNA-21 regulates expression of the PTEN tumor suppressor gene in human hepatocellular cancer. *Gastroenterology* 2007; 133: 647-658.
65. Iorio MV, Visone R, Di Leva G, Donati V, Petrocca F, Casalini P, Taccioli C, Volinia S, Liu CG, Alder H, Calin GA, Menard S, Croce CM. MicroRNA signatures in human ovarian cancer. *Cancer Res* 2007; 67: 8699-8707.
66. Lui WO, Pourmand N, Patterson BK, Fire A. Patterns of known and novel small RNAs in human cervical cancer. *Cancer Res* 2007; 67: 6031-6043.
67. Fulci V, Chiaretti S, Goldoni M, Azzalin G, Carucci N, Tavolaro S, Castellano L, Magrelli A, Citarella F, Messina M, Maggio R, Peragine N, Santangelo S, Mauro FR, Landgraf P, Tuschl T, Weir DB, Chien M, Russo JJ, Ju J, Sheridan R, Sander C, Zavolan M, Guarini A, Foa R, Macino G. Quantitative technologies establish a novel microRNA profile of chronic lymphocytic leukemia. *Blood* 2007; 109: 4944-4951.
68. Jongen-Lavrencic M, Sun SM, Dijkstra MK, Valk PJ, Lowenberg B. MicroRNA expression profiling in relation to the genetic heterogeneity of acute myeloid leukemia. *Blood* 2008; 111: 5078-5085.
69. Navarro A, Gaya A, Martinez A, Urbano-Ispizua A, Pons A, Balague O, Gel B, Abrisqueta P, Lopez-Guillermo A, Artells R, Montserrat E, Monzo M. MicroRNA expression profiling in classic Hodgkin lymphoma. *Blood* 2008; 111: 2825-2832.
70. Krichevsky AM, Gabriely G. miR-21: a small multi-faceted RNA. *J Cell Mol Med* 2009; 13: 39-53.
71. Mattes J, Yang M, Foster PS. Regulation of microRNA by antagomirs: a new class of pharmacological antagonists for the specific regulation of gene function? *Am J Respir Cell Mol Biol* 2007; 36: 8-12.

72. Liu Z, Sall A, Yang D. MicroRNA: an Emerging Therapeutic Target and Intervention Tool. *Int J Mol Sci* 2008; 9: 978-999.
73. Krutzfeldt J, Rajewsky N, Braich R, Rajeev KG, Tuschl T, Manoharan M, Stoffel M. Silencing of microRNAs in vivo with 'antagomirs'. *Nature* 2005; 438: 685-689.
74. Esau C, Davis S, Murray SF, Yu XX, Pandey SK, Pear M, Watts L, Booten SL, Graham M, McKay R, Subramaniam A, Propp S, Lollo BA, Freier S, Bennett CF, Bhanot S, Monia BP. miR-122 regulation of lipid metabolism revealed by in vivo antisense targeting. *Cell Metab* 2006; 3: 87-98.
75. Hendry WJ, 3rd, Sheehan DM, Khan SA, May JV. Developing a laboratory animal model for perinatal endocrine disruption: the hamster chronicles. *Exp Biol Med (Maywood)* 2002; 227: 709-723.
76. Herbst AL, Scully RE, Robboy SJ. Prenatal diethylstilbestrol exposure and human genital tract abnormalities. *Natl Cancer Inst Monogr* 1979: 25-35.
77. Huang WW, Yin Y, Bi Q, Chiang TC, Garner N, Vuoristo J, McLachlan JA, Ma L. Developmental diethylstilbestrol exposure alters genetic pathways of uterine cytodifferentiation. *Mol Endocrinol* 2005; 19: 669-682.
78. Li S, Washburn KA, Moore R, Uno T, Teng C, Newbold RR, McLachlan JA, Negishi M. Developmental exposure to diethylstilbestrol elicits demethylation of estrogen-responsive lactoferrin gene in mouse uterus. *Cancer Res* 1997; 57: 4356-4359.
79. Newbold RR, Bullock BC, McLachlan JA. Testicular tumors in mice exposed in utero to diethylstilbestrol. *J Urol* 1987; 138: 1446-1450.
80. Newbold RR, Bullock BC, McLachlan JA. Lesions of the rete testis in mice exposed prenatally to diethylstilbestrol. *Cancer Res* 1985; 45: 5145-5150.
81. Hendry WJ, 3rd, Zheng X, Leavitt WW, Branham WS, Sheehan DM. Endometrial hyperplasia and apoptosis following neonatal diethylstilbestrol exposure and subsequent estrogen stimulation in both host and transplanted hamster uteri. *Cancer Res* 1997; 57: 1903-1908.
82. Hendry WJ, 3rd, DeBrot BL, Zheng X, Branham WS, Sheehan DM. Differential activity of diethylstilbestrol versus estradiol as neonatal endocrine disruptors in the female hamster (*Mesocricetus auratus*) reproductive tract. *Biol Reprod* 1999; 61: 91-100.
83. Peter ME. Let-7 and miR-200 microRNAs: guardians against pluripotency and cancer progression. *Cell Cycle* 2009; 8: 843-852.

84. Hugo H, Ackland ML, Blick T, Lawrence MG, Clements JA, Williams ED, Thompson EW. Epithelial--mesenchymal and mesenchymal--epithelial transitions in carcinoma progression. *J Cell Physiol* 2007; 213: 374-383.
85. Yang J, Weinberg RA. Epithelial-mesenchymal transition: at the crossroads of development and tumor metastasis. *Dev Cell* 2008; 14: 818-829.
86. Park SM, Gaur AB, Lengyel E, Peter ME. The miR-200 family determines the epithelial phenotype of cancer cells by targeting the E-cadherin repressors ZEB1 and ZEB2. *Genes Dev* 2008; 22: 894-907.
87. Korpala M, Lee ES, Hu G, Kang Y. The miR-200 family inhibits epithelial-mesenchymal transition and cancer cell migration by direct targeting of E-cadherin transcriptional repressors ZEB1 and ZEB2. *J Biol Chem* 2008; 283: 14910-14914.
88. Frankel LB, Christoffersen NR, Jacobsen A, Lindow M, Krogh A, Lund AH. Programmed cell death 4 (PDCD4) is an important functional target of the microRNA miR-21 in breast cancer cells. *J Biol Chem* 2008; 283: 1026-1033.
89. Asangani IA, Rasheed SA, Nikolova DA, Leupold JH, Colburn NH, Post S, Allgayer H. MicroRNA-21 (miR-21) post-transcriptionally downregulates tumor suppressor Pdc4 and stimulates invasion, intravasation and metastasis in colorectal cancer. *Oncogene* 2008; 27: 2128-2136.
90. Chen Y, Knosel T, Kristiansen G, Pietas A, Garber ME, Matsushashi S, Ozaki I, Petersen I. Loss of PDCD4 expression in human lung cancer correlates with tumour progression and prognosis. *J Pathol* 2003; 200: 640-646.
91. Lee S, Bang S, Song K, Lee I. Differential expression in normal-adenoma-carcinoma sequence suggests complex molecular carcinogenesis in colon. *Oncol Rep* 2006; 16: 747-754.
92. Gebeshuber CA, Zatloukal K, Martinez J. miR-29a suppresses tristetraprolin, which is a regulator of epithelial polarity and metastasis. *EMBO Rep* 2009; 10: 400-405.
93. Mott JL, Kobayashi S, Bronk SF, Gores GJ. mir-29 regulates Mcl-1 protein expression and apoptosis. *Oncogene* 2007; 26: 6133-6140.
94. Shi L, Cheng Z, Zhang J, Li R, Zhao P, Fu Z, You Y. hsa-mir-181a and hsa-mir-181b function as tumor suppressors in human glioma cells. *Brain Res* 2008; 1236: 185-193.
95. Cuesta R, Martinez-Sanchez A, Gebauer F. miR-181a regulates cap-dependent translation of p27(kip1) mRNA in myeloid cells. *Mol Cell Biol* 2009; 29: 2841-2851.

96. Mitchell PS, Parkin RK, Kroh EM, Fritz BR, Wyman SK, Pogosova-Agadjanyan EL, Peterson A, Noteboom J, O'Briant KC, Allen A, Lin DW, Urban N, Drescher CW, Knudsen BS, Stirewalt DL, Gentleman R, Vessella RL, Nelson PS, Martin DB, Tewari M. Circulating microRNAs as stable blood-based markers for cancer detection. *Proc Natl Acad Sci U S A* 2008; 105: 10513-10518.